Elsevier Editorial System(tm) for Chemical Engineering Science
Manuscript Draft

Manuscript Number: CES-D-18-02341R1

Title: Influence of CO2 and H2O co-feeding in the NOx abatement by SCR over an efficient Cu-CHA catalyst

Article Type: Research paper

Section/Category: Reaction Engineering, Kinetics and Catalysis

Keywords: Cu-CHA catalyst; copper species; hydrothermal stability; SCR-DeNOx; real conditions; CO2 and H2O co-adsorption

Corresponding Author: Professor Luis J. Alemany, PhD

Corresponding Author's Institution: University of Málaga

First Author: Marina Cortés-Reyes, Ph.D. Student

Order of Authors: Marina Cortés-Reyes, Ph.D. Student; M. Ángeles Larrubia; Concepcion Herrera; Luis J. Alemany

Abstract: Cu-SAPO-34 materials with 2wt% of copper synthesized in one pot with all the copper inside the framework are hydrothermally stable. Copper oxide species were not detected by XRD after thermal and hydrothermal aging at 750 °C. CO2 and H2O molecules are retained on Cu-SAPO catalyst and are related to CO2 adsorption aided by water involving the Cu-species. Copper species coordination is modified by the reaction atmosphere and the species are directly involved in the SCR-process. A decrease in the ammonia storage capacity in the presence of water has been justified due to the cooperative competition between the ammonia and water adsorption and/or CO2 carbonation over the same sites. Higher coordinated Cu species localized inside of CHA-framework, up to a loading close to 4% with this methodology, are highly efficient in the removal of NOx by reaction with ammonia, in the presence of oxygen, water (1.5%) and CO2 (0.3%) as reaction atmosphere. The SCR mechanism is essentially the same as in dry conditions because the Cu2+/Cu+ ions, in equilibrium with H2O+CO2, are the active species in the SCR-reaction. Hydrated-carbonated Cu(II) and Cu(I) species are associated with the redox-chemistry of NOx abatement as responsible for the improvement in the standard SCR; favoring the hindering of ammonia oxidation and nitrate decomposition. In the SCR temperature range, the conversion values registered for this catalyst are higher than 80% with total selectivity to N2.

UNIVERSIDAD
DE MÁLAGA

Facultad de Ciencias
Departamento de Ingeniería Química

Dear Editor of Chemical Engineering Science

We would like to thank all the comments and suggestions for the manuscript entitled “Influence of CO_2 and H_2O co-feeding in the NO_x abatement by SCR over an efficient Cu-CHA catalyst” to be published in Chemical Engineering Science.

We are enclosing herewith the text that has been modified according to the reviewers’ recommendations and a file with the answers to these comments.

Please, consider the revised manuscript for publication in this journal.

Sincerely,

Luis J. Alemany
Departamento de Ingeniería Química. Facultad de Ciencias
Universidad de Málaga

We would like to thank the reviewers for their comments and suggestions. We have clarified some points and have modified the text according to their recommendations in order to make the manuscript acceptable for its publication.

Reviewer #1: The work by Cortés-Reyes et al represents a thorough experimental study in which the effect of CO_2 and H_2O co-feeding on the activity and selectivity of the in the NOx abatement by SCR over an Cu-CHA catalyst is investigated. The topic is of high interest in environmental catalysis in the area of air pollutants treatment and the investigation follows some previous studies published by the same authors and others focused on the same topic. The level of novelty is of the incremental type as no new concepts are introduced here. I suggest publication of the manuscript after taking care of the following minor items.

1) Discussion and conclusions should be improved in their deepness
   According to the reviewer, the text and the conclusions have been modified in order to clarify and delve into the most relevant aspects.

2) How close (or far) are the "quasi-real conditions" as compared with real ones?
   We are working in powder form and similar conditions as other authors (in terms of concentrations, flow, weight of catalyst…). The expression “quasi-real conditions” considers a reaction atmosphere closer to the real that the catalyst can find and is referred to the presence of water and CO_2 in the reaction atmosphere, since they are detected at the outlet gas exhaust of diesel vehicles. Although the concentration of both elements is not the same as in the real conditions is high enough to analyze the influence due to these components. In the manuscript it has been indicated that quasi-real represents the presence of H_2O+CO_2.

3) Some importante chemical engineering aspects, as the influence of mass and heat transfer rates should be addressed, and, if it is possible, sustented with experimental and/or teorethical considerations and calculations.
   To run the experiments the catalyst`s particles are small enough to have kinetic control and avoid diffusive problems. Previous experiments were carried out to calculate the dimensionless numbers and discard any problems, using different weight, flow and particle size and showing that the conversion is constant regardless of W/F ratio. The ratio of the length of the catalytic bed and the diameter of the particle is higher than 100 to ensure ideal plug flow reactor.

Reviewer #3: In their manuscript Cortés-Reyes et al. describe the influence of the presence of CO_2 and water in the feed on the structure of active sites of Cu-SAPO-34 and its performance in deNOx process. The authors present a nice set of catalytic measurements and related TPD and TGA data that are of interest by themselves. Unfortunately, the important conclusions claimed by the authors regarding the coordination and electronic structure of Cu sites are not supported by the data. The authors should either perform additional measurements (e.g. XAS) or calculations that directly support the structural models they suggest, or soften their conclusions, probably orienting them more towards the properties/activity. Therefore, I cannot recommend this manuscript for publication, until the major revisions aimed to address the following concerns are implemented:

1) What is the resulting (Al+P)/Si and Cu/Si ratio of the sample material (analogous to Si/Al and Cu/Al ratio usually reported for silicon-based materials)?

   The (Al+P)/Si and Cu/Si ratio of the materials are 8 and 0.5, respectively, and in consequence Si/Al and Cu/Al ratio are 0.2 and 0.1, respectively. Although the silica content is low, it is in line with the data reported for other authors in the study of SAPO-34 based materials (Martínez-Franco et al., 2014)(Yu et al., 2013). In addition, the copper content, which is in consonance with other authors, has been previously analyzed to ensure the chabazite structure with all the copper inside the framework and is already published in a work focused on the synthesis of this type of materials (Cortés-Reyes et al., 2017). Nevertheless, this value has been included in the text.

2) Based on the data presented in Figure 1, the authors claim that 65% of Cu is in the Cu(I) state. The authors should clarify in which conditions (temperature, atmosphere and pre-treatment) the data were collected. If these data were collected for the as-prepared material at room temperature, they are certainly heavily biased by experimental conditions (UHV + soft X-ray beam + surface sensitivity). Bulk-sensitive Cu K-edge XANES spectroscopy that does not require UHV and does not cause radiation damage (if the intensity of the radiation is reasonably low) evidences that for as-prepared CHA (and not only) zeolites with isolated Cu centers, at RT in air virtually all Cu is in Cu(II) state, and the dominant fraction of Cu ions are surrounded by hydration shell. See for example [Martini et al Chem. Sci., 2017, 8, 6836] or [McEwen et al Catalysis Today 184 (2012) 129-144]. Besides, given the data quality in the inset of the Figure 1, a fit with just one peak instead of two is likely to give similar agreement with the experimental data… Therefore, the conclusions drawn by the authors based on this figure are of dubious value.

   The XPS data have been obtained at room temperature and for the fresh samples as was clarified in the text. As the reviewer suggested, they are certainly heavily biased by experimental conditions and it has been noted. Currently, the author cannot use XANES spectroscopy as other studies, so the conditions and materials are not comparable. A fit of the curve with just one peak the fitting parameters got worse.

   In addition, the presence of Cu^+ species has also been demonstrated by CO adsorption at low temperature (data not shown here) and, in comparison with other catalysts prepared with the modification of the synthesis conditions, the sample used in this work presents a higher Cu^+/Cu^{2+} ratio in fresh conditions. In the previous work (Cortés-Reyes et al., 2017) the study of the physico-chemical properties of this type of materials was detailed in depth and with the intention of not being repetitive we decided not to include it in this manuscript.

3) For the TPD data experiment the pre-treatment conditions should be reported. Also, the data reported in the Figure 3 lack error bars. Since the quantity of the NH_3 adsorbed at high temperature is very low, the associated error for the storage capacity decrease is expected to be quite high.

   The authors appreciate the comment and the pre-treatment conditions have been now included in the text. However, the values represented in Figure 3 correspond to the increment with respect to the values in dry conditions according to the temperature and there is no an accurate determination of adsorption values based in a series of repetition. The trend line is only included with the purpose of increasing the visual effect. The Figure shows how the presence of copper modifies the ammonia storage capacity in incremental terms and, therefore, there is no statistical signification.

4) Discussing the NH_3 oxidation experiment, the authors claim that "Cu^{2+} species do not influence the ammonia oxidation and Cu+ hydrated species are involved". How is this conclusion reached? What is the basis for the claim of having Cu(I)-H_2O species in the sample? I would not expect too much Cu(I) in $H_2O+NH_3+O_2$ atmosphere. Idea of having water as a reducing agent also requires further justification. Has the role of CO_2 been considered?

   The authors agree the comment, because of this fact, the text has been modified, and all the dubious aspects has been clarified in order to properly justify the conclusions.

5) In general, when the authors make the hypotheses regarding the oxidation state or coordination of Cu species in the material, they do not present any data by the techniques (theoretical or experimental) sensitive to the local atomic and electronic structure of Cu species. The only data of such kind that are shown is FTIR, but the interpretation is rather vague, especially given the fact that discriminating between the signals coming form the molecular species adsorbed on Cu and those coordinated to the framework sites is not always an easy task.

   The authors thank the comment and agree in the difficulty of the discrimination between the species adsorbed is not always an easy task. The manuscript has been modified to delve into the species. Nevertheless, although there are XPS, UV-Vis-DR and FTIR data that are more detailed in previous papers, this work is not a physical chemistry study focused on the atomic or theoretical level but on understanding the influence of some reagents, such as water and CO_2, on the SCR performance of these materials. even though

Graphical Abstract

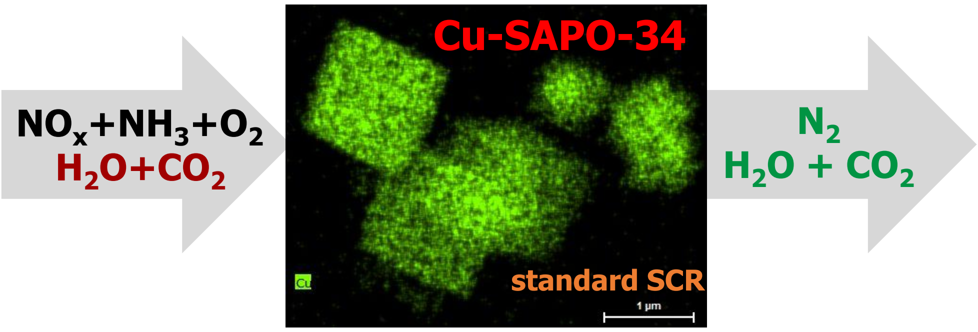

Highlights

- Cu-SAPO-34 with 2wt% of copper is effective in SCR in *quasi*-real conditions
- Cu-CHA model catalyst with copper inside the framework is hydrothermal stable
- Cu(II)-hydrated-carbonated species are responsible for SCR activity improvement
- NH_3 oxidation and nitrate decomposition are hindered under H_2O+CO_2 atmosphere

Influence of CO_2 and H_2O co-feeding in the NO_x abatement by SCR over an efficient Cu-CHA catalyst

Marina Cortés-Reyes, M. Ángeles Larrubia, Concepción Herrera, Luis J. Alemany*

Departamento de Ingeniería Química, Facultad de Ciencias, Campus de Teatinos, Universidad de Málaga, Málaga, E-29071, Spain

**Corresponding author. Tel. and Fax: +34 952131919; e-mail address: luijo@uma.es*

Abstract

Cu-SAPO-34 materials with 2wt% of copper synthesized in one pot with all the copper inside the framework are hydrothermally stable. Copper oxide species were not detected by XRD after thermal and hydrothermal aging at 750 ºC. CO_2 and H_2O molecules are retained on Cu-SAPO catalyst and are related to CO_2 adsorption aided by water involving the Cu-species. Copper species coordination is modified by the reaction atmosphere and the species are directly involved in the SCR-process. A decrease in the ammonia storage capacity in the presence of water has been justified due to the cooperative competition between the ammonia and water adsorption and/or CO_2 carbonation over the same sites. Higher coordinated Cu species localized inside of CHA-framework, up to a loading close to 4% with this methodology, are highly efficient in the removal of NO_x by reaction with ammonia, in the presence of oxygen, water (1.5%) and CO_2 (0.3%) as reaction atmosphere. The SCR mechanism is essentially the same as in dry conditions because the Cu^{2+}/Cu^{+} ions, in equilibrium with H_2O+CO_2, are the active species in the SCR-reaction. Hydrated-carbonated Cu(II) and Cu(I) species are associated with the redox-chemistry of NO_x abatement as responsible for the improvement in the standard SCR; favoring the hindering of ammonia oxidation and nitrate decomposition. In the SCR temperature range, the conversion values registered for this catalyst are higher than 80% with total selectivity to N_2.

Keywords: Cu-CHA catalyst, copper species, hydrothermal stability, SCR-DeNO$_x$, real conditions, CO_2 and H_2O co-adsorption

1. Introduction

Nowadays, the obtaining of zero emission at the outlet gas of a diesel engine is expected to be achieved by the use of coupled technologies NSR-SCR (NO_x Storage and Reduction – Selective Catalytic Reduction) (Bonzi et al., 2010; Can et al., 2015; De La Torre et al., 2016b; Lindholm et al., 2010). Regarding the SCR catalytic bed, zeolitic materials are presented as more suitable NH_3-traps due to their acidity and structure (Colombo et al., 2012a), their high performance at low temperature conditions and their efficiency at high space velocities. Lots of zeolites have been proposed, such as ZSM5 or BETA, with completely different characteristics, framework types or Si/Al ratios, which are important factors for the catalytic properties of the materials (De La Torre et al., 2012; Heo et al., 2011; Kim et al., 2012; Mihai et al., 2014; Mrad et al., 2015). Recently, zeolites with small pore diameter such as chabazite (3.8Å) have been proposed to improve hydrothermal stability with regard to large pore zeolites (Blakeman et al., 2014; Kim et al., 2014; Martínez-Franco et al., 2012), since the pore size is smaller than the diameter of $Al(OH)_3$ and inhibits the dealuminitation process (Blakeman et al., 2014; Leistner and Olsson, 2015). Significant numbers of recent works compare this type of structure with other materials and ensure that SAPO-34 acts effectively in the SCR temperature range and has a better resistance to thermal aging and hydrothermal stability than others, such as SSZ-13, for example (Ma et al., 2014; D. Wang et al., 2015). In addition, a metal is required in the formulation in order to effectively act on the selective catalytic reduction. There are several works in which the differences between the use of iron or copper are detailed (Cheng and Bi, 2014; Colombo et al., 2010). Fe-zeolites usually have less ammonia storage capacity than Cu-zeolites and the latter being more active in the ammonia oxidation process and presenting higher SCR activity at low temperatures, as well as high efficiency in the N_2O decomposition process (Chen et al., 2016; Colombo et al., 2012b; Rutkowska et al., 2015). Therefore, Cu-SAPO-34 can be considered as a promising material for this technology. The content of metal is another key point since a high metal content could lead to extra-framework metal oxide clusters that are active for parallel reactions such as ammonia oxidation or nitrate formation (Brandenberger et al., 2008; De La Torre et al., 2012; Mihai et al., 2014; Shwan et al., 2012). The synthesis method also influences the catalytic activity and the location of the active species. For that reason, in a previous work (Cortés-Reyes et al., 2017) the one-pot synthesis of Cu-SAPO-34 materials with all the copper inside the framework has been widely studied.

The hydrothermal stability of the zeolite and its behaviour in the presence of water are two main concerns in the use of these materials as SCR catalysts. In addition to the beneficial effect of the small pore zeolites on hydrothermal stability, as has been demonstrated in the bibliography, copper species migrate from the external surface into the micropores during hydrothermal treatment at high temperatures (L. Wang et al., 2013), improving the redox ability of the aged Cu/SAPO-34 zeolite and maintaining its acidic properties (Gao et al., 2015; Su et al., 2015). The migration of surface clusters into the cavities also suppresses competitive ammonia oxidation (Liu et al., 2016). During thermal aging the copper ions could be stronger bound as if structural Cu^{2+} were present (Palella et al., 2003). However, several authors have exposed these materials to extreme conditions and have not always obtained good results. The exposure of a Cu-SAPO-34 synthesized in one-pot to a stream with 80% of humidity at 70 ºC produced the collapse of the structure; however, this effect decreased with an increase in copper content, and Cu^{2+} ions seem to be the active species and structure protective agents (J. Wang et al., 2015). *K. Leistner et al*. (Leistner and Olsson, 2015) have also observed similar effects when a Cu/SAPO-34 synthesized by exchanged was exposed to a feed containing water vapor at temperatures below 100 ºC. Nevertheless, the structural changes in the presence of water and after hydrothermal aging are still not clear for catalysts synthesized in one pot with the copper inside.

The study of the SCR reaction in the presence of water and CO_2 simultaneously is also relevant because of the presence of these compounds in exhaust gas. *T. Yu et al.* (Yu et al., 2015) investigated the influence of water and CO_2 in the SCR reaction over a Cu/SAPO-34 synthesized by solid state ion exchange, and observed that the CO_2 did not present a high impact on the conversion, whereas the water presence improved the acidity of Brönsted acid sites and the reducibility of the Cu^{2+} species and, therefore, the SCR activity. The isolated copper species can be modified in the presence of water and converted into a hydrated copper species, which is the active site (Bates et al., 2014). Other authors have shown that Cu^{2+} are the active species via ammonia solvated intermediate modifying the redox-cycle during the process (Gao et al., 2017; Paolucci et al., 2017). However, the influence of the combination of water and CO_2 in the SCR activity and the co-side reactions together with the structural changes and the active metal species have not previously been considered in detail.

Several authors indicate that CO_2 does not influence the SCR activity, whereas the presence of water inhibits the co-side reactions; nevertheless, the effects of the combination of water and CO_2, real conditions, on the hydrothermal stability, the metal species and the SCR performance have not been evaluated. Therefore, the influence of the combination of water and CO_2 remains unclear in the literature and will be addressed in this work, using a Cu-SAPO-34 material that has been directly synthesized with limited extra-framework copper ions. The hydrothermal stability, the active species and their location and the SCR efficiency in water and CO_2 environment are going to be studied.

2. Experimental

2.1. Materials preparation and characterization

SAPO-34 was synthesized by ultrasound assisted hydrothermal method, using the molar gel composition: 2 DEA: 0.6 SiO_2: 1 Al_2O_3: 0.8 P_2O_5: 50 H_2O, keeping the mixtures autoclaved at 200 ºC during 4h. After that, the solid product was filtered and washed with distilled water and dried at 110 ºC overnight. Finally, it was calcined at 550 ºC in air for 5h. The detailed procedure is reported in previous works (Cortés-Reyes et al., 2017, 2016). Copper (2wt%, expressed as copper metal) was incorporated during the synthesis process, by complexation of copper and TEPA (tetraethylenepentamine, Sigma Aldrich) in a molar ratio 1:1.

The catalysts were characterized by different techniques. X-ray Powder Diffraction data were recorded with an X'Pert MPD PRO diffractometer (PANalytical) using Cu Kα1 radiation (λ=1.54059 Å) and a Ge(111) primary monochromator. The X-ray tube worked at 45 kV and 35 mA. The measurements were registered from 5º to 80º (2θ). The composition of the samples was analyzed with the XGT-5000WR Fluorescence spectrometer by X-ray dispersive energy. N_2 adsorption-desorption isotherms were obtained at 77K using a Micromeritics ASAP 2020 Analyzer. Before the analysis, the samples were outgassed in vacuum ($1\cdot10^{-3}$ Pa) for 5h at 453K. UV-Vis Diffuse Reflectance spectra were registered with a T92+UV Spectrophotometer (PG Instruments), equipped with conventional integrating sphere. X-ray Photoelectron Spectra were recorded by using a Physical Electronic 5701 equipped with a PHI 10-360 analyzer using the MgKα X-ray source. The values of binding energy (BE) were referred to the C1s peak (284.8 eV) from the adventitious carbon. All deconvolutions of experimental curves were done with Gaussian-Lorenzian line fitting of varying proportions (60-80%). Adequate and short times of exposure were used in order to diminish the reduction of the copper.

2.2.Hydrothermal stability

The thermal aging and hydrothermal stability were performed by non-isothermal and isothermal protocol in water and water-free environments. The TG-DTA and mass signals were recorded with the SDT Q600 thermobalance from T.A. Instrument connected to a Pfeiffer Prima^{TM} Quadrupole Mass Spectrometer QMS 200. The runs were carried out by steaming 20 mg of the samples with 1% of water in Helium, heating the sample from r.T. to 750 ºC at 10K·min^{-1}, keeping at this temperature for 5h. The analysis of the zeolite structure was studied by XRD Rietveld refinement.

2.3.Catalytic activity

Catalytic tests were performed in a fix bed reactor consisting of a quartz tube, loaded with 60 mg of powder catalyst (100-125 µm) and working without outer diffusional problems. A total flow of 100 cm^{3}min^{-1} (at 1 atm and 0 ºC) was used in all the experiments. The reactor was directly connected to a mass spectrometer (QMS 200, *Pfeiffer Vacuum Prisma^{TM}*) and a micro-gas chromatograph (3000A, *Agilent*) in a parallel arrangement to analyze the reaction products.

Ammonia trap capacity was tested by isothermal ammonia adsorption experiments at different temperatures (150-450 ºC), feeding 750ppm of NH_3 in He for two hours, and then a Helium purge of 90 min was performed in order to remove the physisorbed ammonia. Finally, the sample was heated up to 500 ºC at 15 K·min^{-1}. The catalytic activity for the standard SCR process was studied at different temperatures (150-500 ºC), exposing the sample to a flow that was composed of 750ppm NH_3, 750ppm NO and 3%O_2. To individualize the processes, ammonia oxidation was also studied, introducing a stream of 750ppm of NH_3 and 3% of O_2. All these processes were also performed in 1.5% H_2O+0.3% CO_2 atmosphere.

2.4. CO_2 adsorption study

In order to study the influence of the presence of water in the CO_2 adsorption, TG-MS experiments were carried out in a thermobalance, using 10mg of the sample and 100 ml·min^{-1} of total flow. CO_2 was fed into the chamber in the presence and absence of 1% of H_2O at 200ºC until the saturation of the surface. The product distribution was registered by the QMS

200, *Pfeiffer*. In addition, the same experiments were performed over the self-supported disk of the sample held in a cell connected to a vacuum system that allow the analysis by FTIR. Over the activated surface at 500ºC, 5 torr of CO_2 were adsorbed at 200ºC in dry conditions or over the surface previously hydrated with 3 torr of water. Spectra were recorded at different temperatures.

3. Results and Discussion

The characterization of this type of material has been well detailed in a previous work (Cortés-Reyes et al., 2017). Nevertheless, some relevant data are here explained. The composition of the catalysts was analyzed by XRF. The resulting (Al+P)/Si and Cu/Si ratio of the materials are 8 and 0.5, respectively, and in consequence Si/Al and Cu/Al ratio are 0.2 and 0.1, respectively. These values and the content of each element are quite similar to the theoretical amount used in the synthesis gel composition. The low silica content and copper concentration are in line with the data reported for other authors in the study of SAPO-34 based materials (Martínez-Franco et al., 2014)(Yu et al., 2013).The textural properties for these materials are shown in Table 1. Superficial area and micropore volume values are similar to those reported in the bibliography, in spite of the different copper concentrations, P/Al ratio and the synthesized method (Fan et al., 2013; Leistner and Olsson, 2015; Niu et al., 2016; Shen et al., 2015; Xiang et al., 2016; Yu et al., 2015) and closer to 560 $m^2 \cdot g_{cat}^{-1}$.

Table 1. Textural properties of SAPO-34 and 2Cu-SAPO-34.

Catalyst	**S_{BET} ($m^2 \cdot g^{-1}$)**	**V_μ ($cm^3 \cdot g^{-1}$)**	**V_μ / V_p (%)**
SAPO-34	559	0.24	82
2Cu-SAPO-34	556	0.22	79

These materials are mainly microporous and the incorporation of copper did not destroy the structure. In fact, the micropore/total pore volume ratio for SAPO-34 is 83%, and this value only decreases to 79% with the copper incorporation, maintaining the micropore volume close to 0.22 $cm^3 \cdot g_{cat}^{-1}$.

The species location and distribution for 2Cu-SAPO-34 were analyzed by UV-Vis-DR and XPS. The UV-Vis-DR spectra recorded for both catalysts are displayed in Figure 1 and the profiles are similar to those previously reported (Cortés-Reyes et al., 2017, 2016). For SAPO-

34, a weak peak was detected around 255 nm and as other authors have described (Dang et al., 2009; L. Wang et al., 2013) is associated with the charge transfer (CT) band of the zeolite $(O^{2-} \rightarrow Al^{3+})$ and no additional signals were registered in the whole visible range.

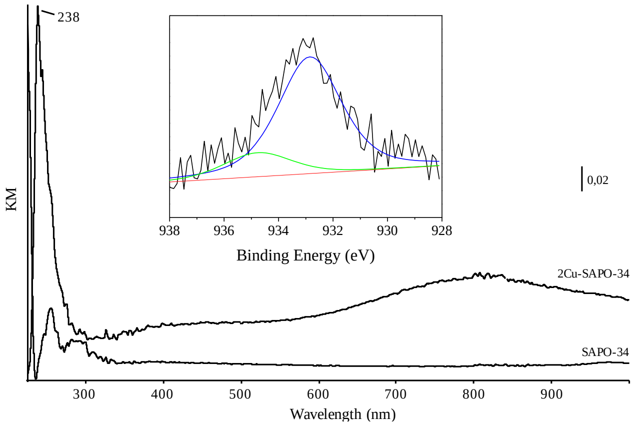

Figure 1. UV-Vis-DR spectra of SAPO-34 and 2Cu-SAPO-34 and XPS of Cu2p region of 2Cu-SAPO-34 (inset).

For 2Cu-SAPO-34, the UV-Vis-DR spectrum is completely different and several intense signals appeared. The most energetic signal was observed at 238 nm and was related to $O^{2-} \rightarrow Cu^{2+}$ ligand to metal charge transfer transition of isolated Cu^{2+} species in agreement with *M. Turco et al.* (Turco et al., 2004). In addition, the broad band centered at 800 nm was assigned to electron d-d transitions of Cu^{2+} ions in distorted octahedral symmetry (Leistner and Olsson, 2015; Turco et al., 2004; L. Wang et al., 2013). Signals related to di-nuclear copper species were barely detected around 425nm. Only Cu^{2+} species can be detected by UV-Vis-DR spectroscopy.

XPS confirms the presence of Cu^{+} species besides Cu^{2+} species. The deconvolution of the Cu2p signal for the fresh catalyst at room temperature is also displayed inside Figure 1. In consonance with other authors (Andonova et al., 2014; Biesinger et al., 2010; Cao et al., 2015; Niu et al., 2016; Pereda-Ayo et al., 2014; L. Wang et al., 2013) that have delved into the XPS analysis of copper, a signal below 933 eV (932.8 eV) and other above (934.8 eV) were observed, as well as the satellite around 943 eV (not shown), necessary to confirm the Cu^{2+} presence. The first represents the 65% of the total amount of copper and, taking into account the Auger parameter, was associated with Cu^{+} species. The latter, 35%, corresponds to isolated Cu^{2+} species. It is noteworthy that these values do not have to coincide with the Cu^{+}/Cu^{2+} ratio under the reaction atmosphere, but as reported by *A. Martini et al.* (Martini et al., 2017) both species are involved in the process. On the catalyst surface, a combination of Cu^{+} and Cu^{2+} oxidized-species was observed, with a higher population of Cu^{+} species. Although the amount of Cu^{+} species could be overestimated due to the fact that is a superficial technique and a partial photoreduction could take place, despite working with short exposure times. However, the values are similar to those reported by other authors (Chen et al., 2014; Wilken et al., 2012) and in consonance with previous works (Cortés-Reyes et al., 2017) where the easy reduction of Cu^{2+} to Cu^{+} was demonstrated.

The hydrothermal stability of the samples analyzed by TG-MS experiments indicated that the evolution of the weight profile and the specific heat flow with the time and the temperature for 2Cu-SAPO-34 are identical regardless of the presence of water in the atmosphere. Moreover, no severe changes in the sample were detected as consequence of the thermal aging. However, the XRD patterns and the unit cell characteristic obtained by Rietveld refinement for the fresh 2Cu-SAPO-34 and after the hydrothermal aging, which are displayed in Figure 2, revealed a slight modification of the structure. A structurally apparent modification was not observed in the diffractogram when CO_2 was present.

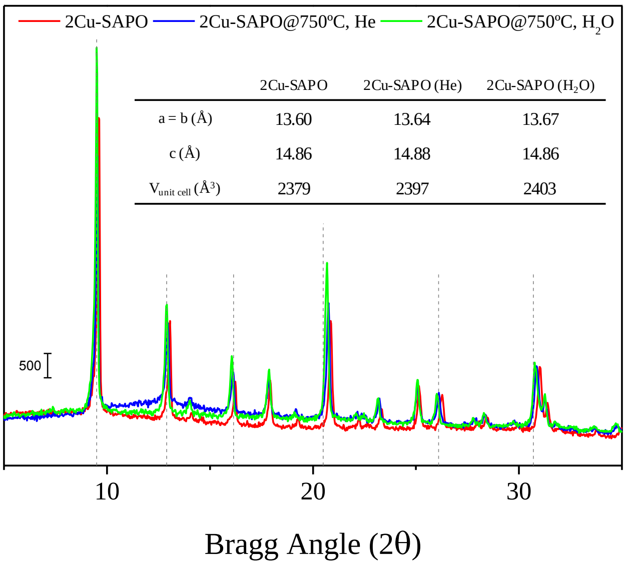

	2Cu-SAPO	2Cu-SAPO (He)	2Cu-SAPO (H_2O)
a = b (Å)	13.60	13.64	13.67
c (Å)	14.86	14.88	14.86
$V_{unit\ cell}$ (Å^3)	2379	2397	2403

Figure 2. X-ray diffraction patterns of 2Cu- SAPO-34 (fresh and after thermal aging in He and in H_2O) and unit cell values (inset table).

In all cases, the XRD patterns showed the diffraction lines associated with chabazite (CHA) structure (JCPDS 01-087-1527) with 2θ signals at 9.4, 12.9, 16.15, 20.5, 26.1 and 30.5º, representative of SAPO-34 samples (Álvaro-Muñoz et al., 2012; Cui et al., 2013; Petitto and Delahay, 2015), with crystal sizes of around 1-5 µm. For the fresh 2Cu-SAPO-34, peaks related to copper oxide were not detected around 35.4 and 38º, as other authors have observed (Gao et al., 2015; D. Wang et al., 2014; Zabilskiy et al., 2015), when the materials are synthesized by ion-exchange method or wet impregnation. The comparison between the 2Cu-SAPO-34 and the wet aged materials did not show a significant difference in the structure and it could even seem that the hydrothermal aging slightly increases the crystallinity. No other copper phases, such as Cu, Cu_2O or CuO, were detected, in line with that reported by *D. Wang et al.* (D. Wang et al., 2015) for a Cu-SAPO-34 synthesized by ion-exchange of a commercial material with 4% of copper or *J. Wang et al.* (Wang et al., 2012) with the same procedure but a lower copper percentage (1%). Nevertheless, as can be observed in the inserted table, the data obtained by Rietveld refinement pointed out an almost insignificant increase in the unit cell volume of 0.8 and 1% for dry and wet conditions, respectively, caused by the hydrothermal treatment. Regarding the distances, the parameter “c” did not suffer any modification, whereas “a” and “b” distances increased, indicating that the cell widens. Other authors have also observed a lattice expansion of the SAPO-34 support after the hydrothermal aging when a 0.9% of copper was incorporated by ion-exchange (L. Wang et al., 2013). Although it is possible to find some work (Cao et al., 2015) that indicates the significantly decrease of crystallinity over a Cu-SAPO-34 synthesized by wetness impregnation, it is generally accepted that the ion exchange method (Duan et al., 2015; Fan et al., 2013; J. Wang et al., 2014) or even the one-pot synthesis with different precursors and protocols (Gao et al., 2015) produce materials with high hydrothermal stability and the copper is well dispersed or may have migrated into the SAPO-34 cavity, next to 8-membered rings. Therefore, hydrated copper in octahedral position and the structure are minimally affected by hydrothermal aging.

In order to study the influence of the water and CO_2 presence in the ammonia adsorption capacity, NH_3-TPD of the different samples activated during 1h at 500ºC in reaction environment were performed in He and in H_2O+CO_2 atmospheres, adsorbing 750 ppm of NH_3 up to saturation (around 2 hours) at several temperatures (150-450 ºC, 100 ºC steps) of the operation range. In all cases, an hour is needed to obtain the completely saturation of the catalyst; however, the breakthrough time and the adsorption rate depend on the temperature and the reaction atmosphere. In dry conditions, an increase in the temperature produces an increment in the adsorption rate and a decrease in the breakthrough time. Nevertheless, in water and CO_2 environment higher values of the breakthrough time were detected, whereas the saturation was faster, increasing the rate with respect to the experiments in Helium.

Values of net adsorbed NH_3 (mmol $NH_3.g_{cat}^{-1}$) calculated subtracting the ammonia desorbed in the purge are shown in Table 2 and are similar to the previously reported (Duan et al., 2015).

Table 2. NH_3 adsorption values (mmol·g_{cat}^{-1}) of NH_3-TPD experiments.

Temperature (ºC)	150	250	350	450
SAPO-34 (He)	0.87	0.55	0.20	0.16
SAPO-34 (H_2O+CO_2)	0.82	0.51	0.18	0.14
2Cu-SAPO-34 (He)	0.87	0.53	0.18	0.11
2Cu-SAPO-34 (H_2O+CO_2)	0.76	0.43	0.11	0.05

As general trend, it is possible to assume that the ammonia adsorption capacity decreases with the increase of temperature, as expected, independently of the copper presence or the reaction atmosphere. When copper is present in the structure, the retention was slightly lower than SAPO-34, indicating that the SAPO-34 is the main responsible for the overall ammonia adsorption capacity. The decrease in the acid sites of SAPO-34 with the loading of copper can be justified due to the substitution of the proton (-Si-OH-Al-) of the support by Cu^{2+} species (Duan et al., 2015; Wang et al., 2012). The presence of water and CO_2 in the reaction atmosphere caused a decrease in the ammonia adsorption capacity, being more evident for 2Cu-SAPO-34. Some authors (Yu et al., 2015) have observed an increase in the adsorbed NH_3 contents by an increment in the acid density, whereas in general a decrease in the ammonia storage in the presence of water has been justified due to the cooperative competition between the ammonia and water adsorption and/or CO_2 carbonation over the same sites (Leistner and Olsson, 2015). The data of the reduction of the ammonia storage capacity due to the presence of water and CO_2, expressed as percentage, are represented in Figure 3.

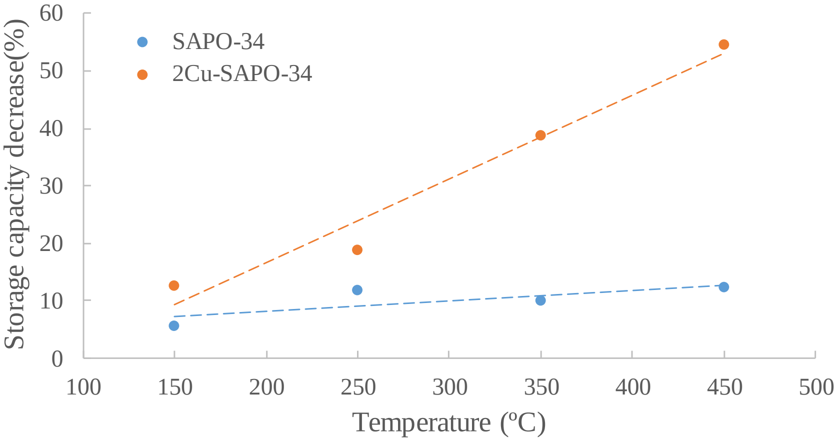

Figure 3. Ammonia storage capacity decrease percentage in the presence of 1.5%H_2O and 0.3% CO_2 in relation to dry conditions.

These data indicated that the adsorption capacity seems not to be further affected by temperature for the SAPO-34 material, since the slope of the fitted data according to temperature remains close to $0.1.10^{-3}$. Nevertheless, the slope registered for 2Cu-SAPO-34 increased ten times with respect to Cu-free catalyst. This fact is associated with the impact of H_2O+CO_2 combination on the NH_3 adsorption, related to overall acidity behavior of copper species. Therefore, the reduction of acid sites corresponds to the partial occupancy of sites by some kind of hydro-carbonation of Cu species. The latter is responsible for the expansion of the NH_3-breakthrough-time and the faster saturation rate. Even though the ammonia storage capacity can decrease in the presence of water and CO_2, because of the modification of the acid centers in agreement with other authors (Busca et al., 1998; Su et al., 2015; Wang et al., 2012; Yu et al., 2015), a high capacity value was kept, making its use as ammonia trap possible.

The SCR activity was studied in a flow reactor, feeding 750ppm of NH_3, 750ppm of NO and 3% of O_2 in He (dry conditions) or 1.5% of H_2O and 0.3% of CO_2 (mix-conditions). In Figure 4, the SCR activity parameters, such as ammonia and NO conversion and N_2, N_2O and NO_2 selectivity, are displayed in the studied temperature range (150-500 °C) for the Cu-free and Cu-SAPO-34 catalysts. Regarding the SAPO-34 behavior in dry conditions, the NO-conversion is low registering the maximum value at 250 °C close to 30%. Above this temperature, the NO conversion decreased below zero, pointing out that NO production occurs. However, the NH_3 conversion increased with the temperature up to the total conversion above 300 °C. So, the ammonia reacts with the available oxygen, via ammonia oxidation in gas phase, producing not only nitrogen, but also N_2O, NO and NO_2. It should also be noted that high levels of N_2O formation are measured around 250 ºC and its production is related to surface nitrate decomposition. This agrees with those data reported by *T. Yu et al.* (Yu et al., 2015) for a hydrothermally synthesized SAPO-34 where they observed low NO conversion values, ammonia oxidation from 300 ºC and N_2O generation with a maximum at 320 ºC. In SCR-mix conditions (i.e. H_2O+CO_2), NO and NH_3 conversion values and selectivity trends are almost identical to dry conditions, indicating that the H_2O+CO_2 combination does not affect the already low SCR activity for SAPO-34.

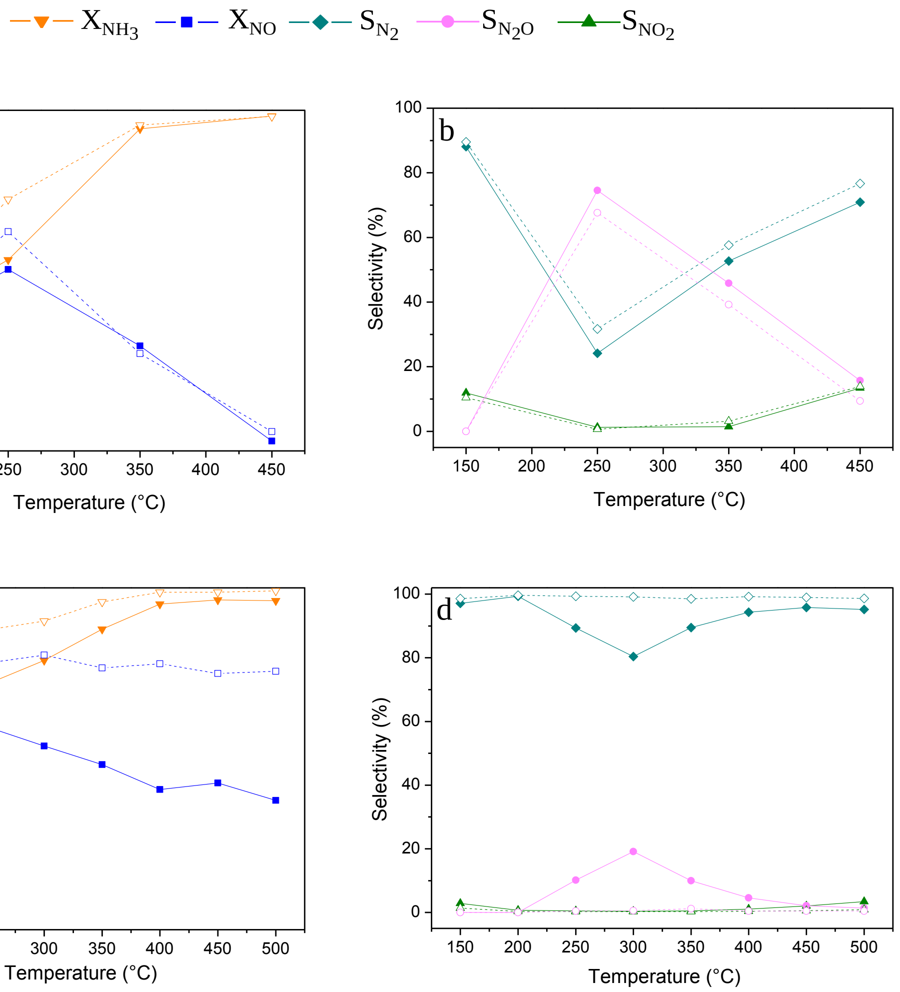

Figure 4. SCR activity parameters (conversion and selectivity) for SAPO-34 (a, b) and 2Cu-SAPO-34 (c, d) in He (solid lines) and in H_2O + CO_2 atmosphere (dotted lines)

For 2Cu-SAPO-34, the profiles of conversion and selectivity in dry conditions are displayed in Figures 4c and 4d and indicated that there are several reactions taking place. At low temperatures (up to 200 ºC), the conversion of NH_3 and NO was stoichiometric producing nitrogen and water, which means that the standard SCR occurs. In the SCR temperature range, between 200 and 400 ºC, and up to 500 ºC, the NH_3 conversion was higher than NO conversion, indicating another via of ammonia consumption without NO intervention, which is the ammonia oxidation. *D. Wang et al.* (D. Wang et al., 2013) also observed the NH_3 oxidation together with a decrease in the NO conversion at temperature higher than 200 ºC with a copper exchange commercial SAPO-34. Furthermore, there was a significant N_2O formation with a maximum at 300 ºC associated with the direct nitrate decomposition, which occurs in this temperature range. By in situ-FTIR analysis (Cortés-Reyes et al., 2016) and dynamic pulse experiments, the adsorption of NO over this catalyst has been carried out in dry conditions. For this catalyst, nitrate formation was observed and at temperature values higher than 300ºC, their decomposition with N_2O formation. These experiments are in accordance with *T. Yu et al.* (Yu et al., 2014) who reported that the decomposition of nitrates produces N_2O, since it is the most probably side reaction.

From the activity data, it has been confirmed that the presence of H_2O and CO_2 in the reaction atmosphere provoked a significant modification in the processes that take place. At low SCR-temperature range (<200 ºC) the conversions of NO and NH_3 were almost identical with total nitrogen production (Fig. 4c and 4d). So, the standard SCR is the main reaction with a NO and NH_3 conversion of 75% and a complete selectivity to N_2. In the temperature range between 200 and 500 ºC, the NH_3 conversion remained higher than that of NO, pointing out that besides the standard SCR, the ammonia oxidation occurs in minor extent that registered in dry conditions; both lead to N_2 selective production. It is noteworthy that N_2O was not detected in the temperature range, meaning that the side-reactions with undesired compounds production are also hindered, enhancing the SCR activity due to the inhibition of N_2O production (Busca et al., 1998). Other authors (Yu et al., 2015) indicated that CO_2 presence in the feeding apparently did not influence the SCR activity for a Cu-SAPO-34 prepared in two steps at low Cu loading (<1%) incorporated by ion-exchanged, whereas the H_2O addition improved the NH_3-SCR activity and the NO_2 and N_2O selectivity values decreased. *U. De La Torre et al.* (De La Torre et al., 2016a) have observed an increase in the N_2O production at intermediate temperatures after the hydrothermal aging and have related it to the partial loss of the acidity and the micropore volume of the catalysts. On the contrary, in the presence of water and CO_2, despite the variation of the acidity, the structure was not modified and the N_2O production was completely hindered, thence, the inhibition of a reaction responsible for the N_2O formation takes place, which could be related to the chemical environment of the copper species being changed. H_2O and CO_2 combination should be responsible for the improved NH_3-SCR performance over the model 2Cu-SAPO-34 catalyst, due to the inhibition of side reaction such as the nitrate decomposition route and ammonia oxidation.

In order to confirm the beneficial effect of H_2O+CO_2 combination on the SCR-DeNO$_x$, ammonia oxidation experiments were carried out and compared in dry and wet conditions, both of them were also studied in the same reactor, feeding 750 ppm of NH_3 + 3% of O_2, being the results shown in Figure 5.

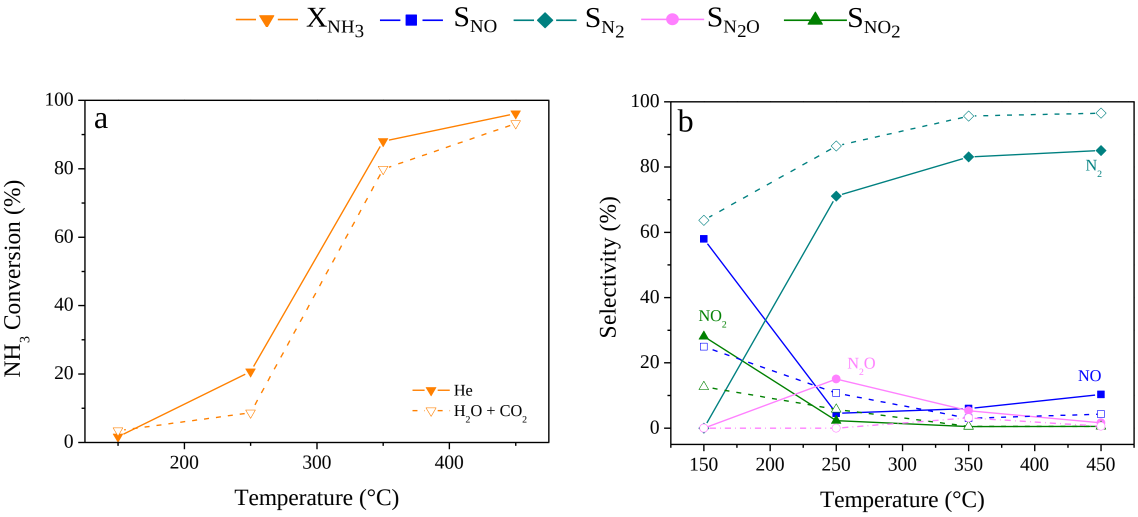

Figure 5. NH_3 oxidation conversion (a) and selectivity (b) values vs temperature in He (solid lines) and in H_2O+CO_2 (dotted lines) atmospheres for 2Cu-SAPO-34.

The NH_3 conversion increased with the temperature independently of the atmosphere, with values higher than 90% at temperatures above 300 ºC in dry conditions. At low temperatures, the conversion values were insignificant and, therefore, the selectivity values cannot be considered as representative, since the concentrations of the products were minimal. Around 250 ºC, there was a slight formation of N_2O, which can contribute to the N_2O production detected in the SCR experiments. However, the increase of the temperature did not produce a higher amount of this component, and the maximum detected in the previous experiments has to involve another process.

The presence of water and CO_2 not only inhibits the ammonia oxidation, but also increases the nitrogen selectivity, in agreement with the observed in the SCR conditions. In addition, there was no production of N_2O in the whole temperature range because the centers responsible for nitrate formation are blocked as has been explained above. It is noteworthy that several authors have detected NO as the main product of the oxidation, because of its formation in CuO species (J. Wang et al., 2014), which are not present in this one-pot synthesized material. Regarding the inhibition of ammonia oxidation in presence of water and CO_2 in this material, Cu^+ species would be stabilized in Cu^+-hydrated-carbonated form and, probably, these species inhibit ammonia oxidation. These data are in accordance with that reported by other authors (D. Wang et al., 2014; J. Wang et al., 2014; Yu et al., 2015), in which the Cu_xO_y clusters or Cu^+ species responsible for the ammonia oxidation are reduced as consequence of the water interaction.

In order to study the dependence of the water presence in the carbonation of the materials, TG-MS isothermal experiments were carried out adsorbing CO_2 in the presence and absence of water until the saturation of the sample. It should be noticed that CO_2 was not adsorbed onto the catalyst in the absence of water, indicating that in dry conditions, the catalyst is not carbonated, regardless of the copper species. The TG profile after the water adsorption is displayed in Figure 6 and presents a typical adsorption curve, which after 100 min reached a weight gain of about 0.35% of its initial weight in consonance with the signals obtained by mass spectrometry.

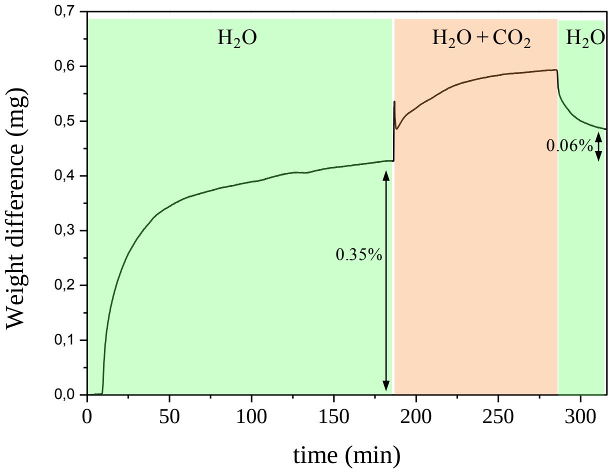

Figure 6. Weight difference profile along the time for water and CO_2 adsorption over 2Cu-SAPO-34 registered by TGA at 200 ºC.

In Figure 7, the CO_2 profile during the adsorption is represented for both conditions. In water environment (wet), the consumption of CO_2 was detected due to the CO_2 adsorption over the previously hydrated sample; different from the dry adsorption that did not produce a net CO_2 adsorption. It is noteworthy that the coadsorption at 200ºC of both compounds, H_2O and CO_2, produced a storage of around 40 µmol of $CO_2 \cdot g_{cat}^{-1}$, when the catalyst was previously hydrated with 75 µmol of $H_2O.g_{cat}^{-1}$.

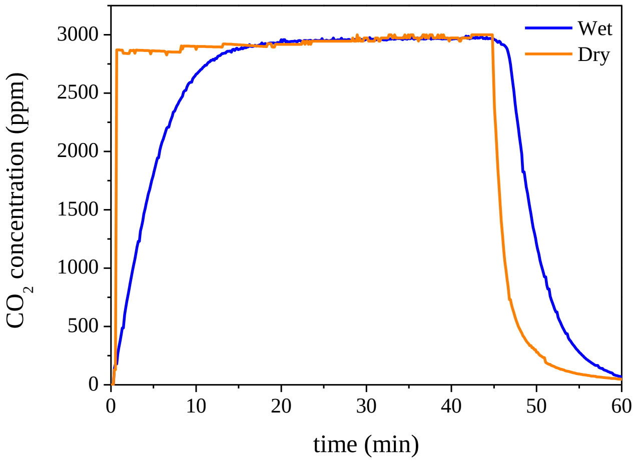

Figure 7. CO_2 profile during the adsorption in the presence of water (wet) and He (dry).

A comprehensive explanation about how CO_2 and H_2O molecules are retained on Cu-SAPO-34 catalyst should be related to CO_2 adsorption aided by water involving Cu-species. Copper species (in oxidation state (I) and (II)) are stabilized and chemically modified in this environment and they are directly involved in the SCR-process, through the carbonated-hydrated species, produced in these conditions.

The modification of the species due to the presence of water and CO_2 was also analyzed by FTIR and the spectra of the adsorption of CO_2, water and H_2O+CO_2 at 200 ºC with the subtraction of the activated sample are represented in Figure 8; prior to the adsorption, the surface was activated at 500ºC for 2h under vacuum to completely clean the surface.

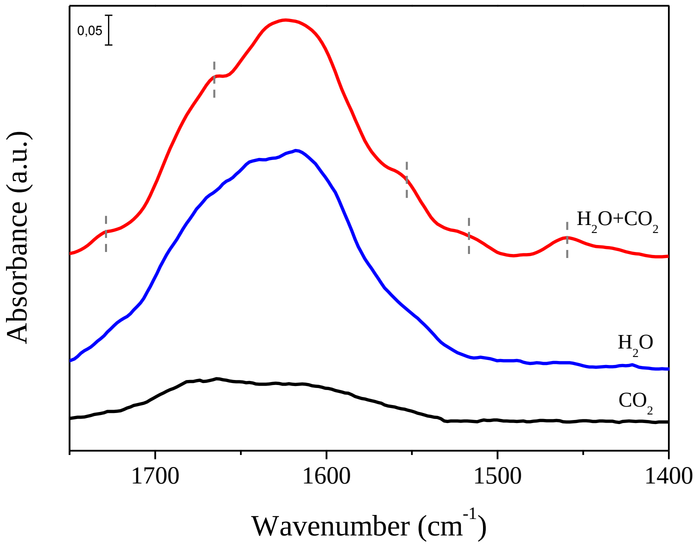

Figure 8. FTIR spectra after adsorption and outgassing at 200 ºC of CO_2, water and CO_2 and water over 2Cu-SAPO-34.

The adsorption of CO_2 barely produced the modification of the spectra, in consonance with the TG-MS experiments in which the carbon dioxide was not adsorbed. For the water adsorption, the main signal was broad and detected in the region between 1800 and 1500 cm^{-1}, with a maximum at 1620 cm^{-1}, due to the bending mode of water adsorbed onto the surface of the catalyst (Bordiga et al., 2005). The hydrophilic character of SAPO-34 materials is already known (Regli et al., 2005)(Bonaccorsi et al., 2013) and agree with the data obtained in the thermobalance where a weight gain of 0.35% of its initial value has been observed when copper is present. The adsorption of CO_2 over the hydrated sample caused the appearance of a broad and less symmetrical signal with apparent maxima around 1730, 1670, 1550, 1520 and 1460 cm^{-1} superimposed to the band related to the presence of water. Those signals are associated with the formation of bridging, bidentate, monodentate, polydentate and free carbonate species (Danon et al., 2011; Köck et al., 2013; Montanari and Busca, 2008; Villarreal et al., 2017; Westermann et al., 2017, 2015), which were not detected over the sample in dry conditions. The wide variety of carbonate species can be related to several centers, such as copper in different oxidation states previously hydrated and located in the 8 or 6 membered rings, which cannot be completely distinguished. The evolution of the species with the increase in temperature without evacuation was studied by FTIR and the resulting spectra are shown in Figure 9, where the strength and population of these species is evidenced.

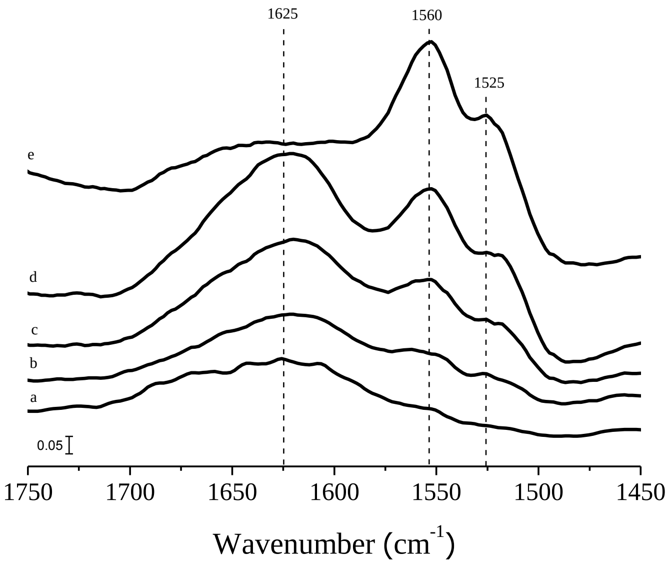

Figure 9. FTIR spectra over 2Cu-SAPO-34 after the co-adsorption of H_2O and CO_2 at a) 200, b) 300, c) 350 and d) 400 ºC and e) after outgassing the sample.

At higher temperatures, signals with maximum at 1625, 1560 and 1525 cm^{-1} that correspond to carbonate-like or hydrogencarbonate species are still present. These signals remained until evacuation of around 400 ºC, indicating similar strength to adsorbed ammonia species (Cortés-Reyes et al., 2016). It is remarkable to note that the carbonation capacity further depends on the hydration of the sample. The interaction between copper species and water and CO_2 would be associated with isolated Cu^+ species preferentially in tetrahedral coordination (Bates et al., 2014), as Cu^+-H_2O-CO_2 stabilized species and Cu^{2+} species in octahedral coordination as part of the structure, which would be prone to higher hydration and carbonation producing azurite-like species ($Cu_3(CO_3)_2(OH)_2$) (Gao et al., 2013; Godiksen et al., 2014).

The mechanism of SCR of NO with NH_3 in presence of O_2, H_2O and CO_2 essentially does not change and the presence of both Cu^+ and Cu^{2+} ions are also visible under SCR conditions. Standard SCR is associated with Cu-redox chemistry requiring NH_3 and NO+O_2; in similar way that in H_2O+CO_2 atmosphere, where the Cu(II) and Cu(I) species are in equilibrium, as copper hydrated carbonated species; these types of copper species are able to react with NO and ammonia to form nytrosil and NH_4^+ intermediates as key species in the SCR process (Cortés-Reyes et al., 2016).

The efficiency of Cu-CHA catalyst in the SCR-DeNO$_x$ process in H_2O+CO_2 conditions is also associated with the increase in the nitrogen selectivity due to the decrease of the N_2O production. In agreement with the bibliography (Grossale et al., 2009), the N_2O formation is caused by the decomposition of surface nitrates, which in the presence of water and CO_2 increase their stability and inhibit their decomposition or the centers for their production are covered. In these conditions, dinuclear Cu species that facilitate nitrate decomposition with N_2O formation were not detected. The reducibility of the tetrahedral Cu^{2+} species is favored in the presence of water, as has been observed over Cu-SSZ-13 synthesized by ion-exchange (Hun Kwak et al., 2012), probably due to the fact that the migration of copper species decreases the bond strength between Cu^{2+} species and the oxygen atoms of the SAPO-34 skeleton and makes the reduction of the adsorbed species faster. In the simultaneous presence of CO_2 and water, Cu^{+} and Cu^{2+}-hydrated-carbonated higher coordination species located within CHA-structure, are visible and are responsible for the improvement in the standard SCR. Additionally in these conditions and at low temperatures the standard NH_3-SCR reaction is much faster than ammonia oxidation and was the main reaction in any atmosphere, increasing the conversion values in the presence of water+CO_2. At high temperatures, N_2O formation was observed due to the nitrate decomposition, and ammonia oxidation took place largely under dry conditions. However, the presence of water+CO_2 modifies the Cu-speciation with the formation of Cu^{2+}-H_2O-CO_2 and Cu^{+}-H_2O-CO_2 species that are apparently responsible for the SCR-performance because these species favor the inhibition of coupled processes, being completely selective to nitrogen in the whole SCR range.

4. Conclusions

Cu-SAPO-34 model SCR catalysts synthesized in one pot with 2wt% of copper inside the framework are hydrothermally stable and the migration of copper to octahedral coordination slightly widens the unit cell. CO_2 is not adsorbed in dry conditions; however, 40 µmol of $CO_2 \cdot g_{cat}^{-1}$ can be adsorbed over the previously hydrated catalyst, via different carbonate species, such as bridging, bidentate, monodentate or polydentate when copper is present in the formulation. NH_3-TPD experiments under different atmospheres allowed the detection of a decrease in the ammonia storage capacity in the presence of water+CO_2, which has been justified due to the cooperative competition between the ammonia and water adsorption and/or CO_2 carbonation over the same sites. Copper species coordination is modified by the reaction atmosphere and the species are directly involved in the redox chemistry of the SCR-process. This material has proven to be efficiently selective to nitrogen because of the inhibition of nitrate decomposition and, in addition, ammonia oxidation is hindered in the SCR technology under *quasi*-real conditions (1.5%H_2O+0.3%CO_2) in the whole SCR operation temperature range; ensuring NO_x conversion values around 80% and total selectivity to nitrogen.

Acknowledgements

MCR acknowledges the Spanish Ministry of Education, Culture and Sport (FPU12/03826) for the FPU grant and Universidad de Málaga. Campus de Excelencia Internacional Andalucía Tech. The authors want to thank the financial support of the CTQ 2013-47853R Project. Special thanks to Prof Luca Lietti and the LCCP Research Group from Politecnico di Milano for the replication of the catalytic activity experiments in their facilities.

References

Álvaro-Muñoz, T., Márquez-Álvarez, C., Sastre, E., 2012. Use of different templates on SAPO-34 synthesis: Effect on the acidity and catalytic activity in the MTO reaction. Catal. Today 179, 27–34. https://doi.org/10.1016/j.cattod.2011.07.038

Andonova, S., Vovk, E., Sjöblom, J., Ozensoy, E., Olsson, L., 2014. Chemical deactivation by phosphorous under lean hydrothermal conditions over Cu/BEA NH3-SCR catalysts. Appl. Catal. B Environ. 147, 251–263. https://doi.org/10.1016/j.apcatb.2013.08.041

Bates, S.A., Verma, A.A., Paolucci, C., Parekh, A.A., Anggara, T., Yezerets, A., Schneider, W.F., Miller, J.T., Delgass, W.N., Ribeiro, F.H., 2014. Identification of the active Cu site in standard selective catalytic reduction with ammonia on Cu-SSZ-13. J. Catal. 312, 87–97. https://doi.org/10.1016/j.jcat.2014.01.004

Biesinger, M.C., Lau, L.W.M., Gerson, A.R., Smart, R.S.C., 2010. Resolving surface chemical states in XPS analysis of first row transition metals, oxides and hydroxides: Sc, Ti, V, Cu and Zn. Appl. Surf. Sci. 257, 887–898. https://doi.org/10.1016/j.apsusc.2010.07.086

Blakeman, P.G., Burkholder, E.M., Chen, H.-Y., Collier, J.E., Fedeyko, J.M., Jobson, H., Rajaram, R.R., 2014. The role of pore size on the thermal stability of zeolite supported Cu SCR catalysts. Catal. Today 231, 56–63. https://doi.org/10.1016/j.cattod.2013.10.047

Bonaccorsi, L., Calabrese, L., Freni, A., Proverbio, E., 2013. Hydrothermal and microwave synthesis of SAPO (CHA) zeolites on aluminium foams for heat pumping applications. Microporous Mesoporous Mater. 167, 30–37. https://doi.org/10.1016/j.micromeso.2012.06.006

Bonzi, R., Lietti, L., Castoldi, L., Forzatti, P., 2010. NOx removal over a double-bed NSR-SCR reactor configuration. Catal. Today 151, 376–385. https://doi.org/10.1016/j.cattod.2010.02.003

Bordiga, S., Regli, L., Lamberti, C., Zecchina, A., Bjørgen, M., Lillerud, K.P., 2005. FTIR Adsorption Studies of H2O and CH3OH in the Isostructural H-SSZ-13 and H-SAPO-34 : Formation of H-Bonded Adducts and Protonated Clusters. J. Phys. Chem. B 109, 7724–7732.

Brandenberger, S., Kröcher, O., Tissler, A., Althoff, R., 2008. The State of the Art in Selective Catalytic Reduction of NOx by Ammonia Using Metal-Exchanged Zeolite Catalysts, Catalysis Reviews. https://doi.org/10.1080/01614940802480122

Busca, G., Lietti, L., Ramis, G., Berti, F., 1998. Chemical and mechanistic aspects of the selective catalytic reduction of NOx by ammonia over oxide catalysts: A review. Appl. Catal. B Environ. 18, 1–36. https://doi.org/10.1016/S0926-3373(98)00040-X

Can, F., Courtois, X., Berland, S., Seneque, M., Royer, S., Duprez, D., 2015. Composition dependent performance of alumina-based oxide supported WO3 catalysts for the NH3-SCR reaction and the NSR + SCR coupled process. Catal. Today 257, 41–50. https://doi.org/10.1016/j.cattod.2015.03.024

Cao, Y., Zou, S., Lan, L., Yang, Z., Xu, H., Lin, T., Gong, M., Chen, Y., 2015. Promotional effect of Ce on Cu-SAPO-34 monolith catalyst for selective catalytic reduction of NOx with ammonia. J. Mol. Catal. A Chem. 398, 304–311. https://doi.org/10.1016/j.molcata.2014.12.020

Chen, B., Xu, R., Zhang, R., Liu, N., 2014. Economical way to synthesize SSZ-13 with abundant ion-exchanged Cu+ for an extraordinary performance in selective catalytic reduction (SCR) of NOx by ammonia. Environ. Sci. Technol. 48, 13909–13916. https://doi.org/10.1021/es503707c

Chen, P., Rauch, D., Weide, P., Schönebaum, S., Simons, T., Muhler, M., Moos, R., Simon, U., 2016. The effect of Cu and Fe cations on NH3-supported proton transport in

DeNOx-SCR zeolite catalysts. Catal. Sci. Technol. https://doi.org/10.1039/C6CY00452K

Cheng, X., Bi, X.T., 2014. A review of recent advances in selective catalytic NOx reduction reactor technologies. Particuology 16, 1–18. https://doi.org/10.1016/j.partic.2014.01.006

Colombo, M., Nova, I., Tronconi, E., 2012a. Detailed kinetic modeling of the NH3–NO/NO2 SCR reactions over a commercial Cu-zeolite catalyst for Diesel exhausts after treatment. Catal. Today 197, 243–255. https://doi.org/10.1016/j.cattod.2012.09.002

Colombo, M., Nova, I., Tronconi, E., 2012b. NO2 adsorption on Fe- and Cu-zeolite catalysts: The effect of the catalyst red–ox state. Appl. Catal. B Environ. 111–112, 433–444. https://doi.org/10.1016/j.apcatb.2011.10.031

Colombo, M., Nova, I., Tronconi, E., 2010. A comparative study of the NH3-SCR reactions over a Cu-zeolite and a Fe-zeolite catalyst. Catal. Today 151, 223–230. https://doi.org/10.1016/j.cattod.2010.01.010

Cortés-Reyes, M., Finocchio, E., Herrera, C., Larrubia, M.A., Alemany, L.J., Busca, G., 2017. A study of Cu-SAPO-34 catalysts for SCR of NOx by ammonia. Microporous Mesoporous Mater. 241, 258–265. https://doi.org/10.1016/j.micromeso.2016.11.032

Cortés-Reyes, M., Herrera, M.C., Larrubia, M.A., Alemany, L.J., 2016. Fast ultrasound assisted synthesis of Cu-SAPO-34 for SCR application. Int. J. Innov. Res. Sci. Eng. Technol. 5, 5540–5550. https://doi.org/10.15680/IJIRSET.2016.0504189

Cui, Y., Zhang, Q., He, J., Wang, Y., Wei, F., 2013. Pore-structure-mediated hierarchical SAPO-34: Facile synthesis, tunable nanostructure, and catalysis applications for the conversion of dimethyl ether into olefins. Particuology 11, 468–474. https://doi.org/10.1016/j.partic.2012.12.009

Dang, T.T.H., Zubowa, H.-L., Bentrup, U., Richter, M., Martin, A., 2009. Microwave-assisted synthesis and characterization of Cu-containing AlPO4-5 and SAPO-5. Microporous Mesoporous Mater. 123, 209–220. https://doi.org/10.1016/j.micromeso.2009.04.003

Danon, A., Stair, P.C., Weitz, E., 2011. FTIR Study of CO2 Adsorption on Amine-Grafted SBA-15: Elucidation of Adsorbed Species. J. Phys. Chem. C 115, 11540–11549.

De La Torre, U., Pereda-Ayo, B., González-Velasco, J.R., 2012. Cu-zeolite NH3-SCR catalysts for NOx removal in the combined NSR–SCR technology. Chem. Eng. J. 207–208, 10–17. https://doi.org/10.1016/j.cej.2012.06.092

De La Torre, U., Pereda-Ayo, B., Moliner, M., González-Velasco, J.R., Corma, A., 2016a. Cu-zeolite catalysts for NOx removal by selective catalytic reduction with NH3 and coupled to NO storage/reduction monolith in diesel engine exhaust aftertreatment systems. Appl. Catal. B Environ. 187, 419–427. https://doi.org/10.1016/j.apcatb.2016.01.020

De La Torre, U., Urrutxua, M., Pereda-Ayo, B., González-Velasco, J.R., 2016b. On the Cu species in Cu/beta catalysts related to DeNOx performance of coupled NSR-SCR technology using sequential monoliths and dual-layer monolithic catalysts. Catal. Today 273, 72–82. https://doi.org/10.1016/j.cattod.2016.02.054

Duan, Y., Wang, J., Yu, T., Shen, M., Wang, J., 2015. The role and activity of various adsorbed ammonia species on Cu/SAPO-34 catalyst during passive-SCR process. RSC Adv. 5, 14103–14113. https://doi.org/10.1039/c4ra13984d

Fan, S., Xue, J., Yu, T., Fan, D., Hao, T., Shen, M., Li, W., 2013. The effect of synthesis methods on Cu species and active sites over Cu/SAPO-34 for NH3-SCR reaction. Catal. Sci. Technol. 3, 2357–2364. https://doi.org/10.1039/c3cy00267e

Gao, F., Kwak, J.H., Szanyi, J., Peden, C.H.F., 2013. Current understanding of Cu-Exchanged Chabazite molecular sieves for use as commercial diesel engine DeNOx catalysts. Top. Catal. 56, 1441–1459. https://doi.org/10.2800/51626

Gao, F., Mei, D., Wang, Y., Szanyi, J., Peden, C.H.F., 2017. Selective Catalytic Reduction over Cu/SSZ-13: Linking Homo- and Heterogeneous Catalysis. J. Am. Chem. Soc. 139, 4935–4942. https://doi.org/10.1021/jacs.7b01128

Gao, F., Walter, E.D., Washton, N.M., Szanyi, J., Peden, C.H.F., 2015. Synthesis and evaluation of Cu/SAPO-34 catalysts for NH3-SCR 2 : Solid-state ion exchange and one-pot synthesis. Appl. Catal. B Environ. 162, 501–514. https://doi.org/10.1016/j.apcatb.2014.07.029

Godiksen, A., Stappen, F.N., Vennestrøm, P.N.R., Giordanino, F., Rasmussen, S.B., Lundegaard, L.F., Mossin, S., 2014. Coordination Environment of Copper Sites in Cu-CHA Zeolite Investigated by Electron Paramagnetic Resonance. J. Phys. Chem. C 118, 23126–23138. https://doi.org/10.1021/jp5065616

Grossale, A., Nova, I., Tronconi, E., 2009. Ammonia blocking of the “Fast SCR” reactivity over a commercial Fe-zeolite catalyst for Diesel exhaust aftertreatment. J. Catal. 265, 141–147. https://doi.org/10.1016/j.jcat.2009.04.014

Heo, I., Lee, Y., Nam, I.-S., Choung, J.W., Lee, J.-H., Kim, H.-J., 2011. Effect of hydrocarbon slip on NO removal activity of CuZSM5, FeZSM5 and V2O5/TiO2 catalysts by NH3. Microporous Mesoporous Mater. 141, 8–15. https://doi.org/10.1016/j.micromeso.2010.02.005

Hun Kwak, J., Zhu, H., Lee, J.H., Peden, C.H.F., Szanyi, J., 2012. Two different cationic positions in Cu-SSZ-13? Chem. Commun. 48, 4758–4760. https://doi.org/10.1039/c2cc31184d

Kim, Y.J., Kwon, H.J., Heo, I., Nam, I.-S., Cho, B.K., Choung, J.W., Cha, M.-S., Yeo, G.K., 2012. Mn–Fe/ZSM5 as a low-temperature SCR catalyst to remove NOx from diesel engine exhaust. Appl. Catal. B Environ. 126, 9–21. https://doi.org/10.1016/j.apcatb.2012.06.010

Kim, Y.J., Lee, J.K., Min, K.M., Hong, S.B., Nam, I.-S., Cho, B.K., 2014. Hydrothermal stability of CuSSZ13 for reducing NOx by NH3. J. Catal. 311, 447–457. https://doi.org/10.1016/j.jcat.2013.12.012

Köck, E.-M., Kogler, M., Bielz, T., Klötzer, B., Penner, S., 2013. In Situ FT-IR Spectroscopic Study of CO2 and CO Adsorption on Y2O3 ,ZrO2, and Yttria-Stabilized ZrO2. J. Phys. Chem. C 117, 17666–17673.

Leistner, K., Olsson, L., 2015. Deactivation of Cu/SAPO-34 during low-temperature NH3-SCR. Appl. Catal. B Environ. 165, 192–199. https://doi.org/10.1016/j.apcatb.2014.09.067

Lindholm, A., Sjövall, H., Olsson, L., 2010. Reduction of NOx over a combined NSR and SCR system. Appl. Catal. B Environ. 98, 112–121. https://doi.org/10.1016/j.apcatb.2010.05.019

Liu, X., Wu, X., Weng, D., Si, Z., Ran, R., 2016. Evolution of copper species on Cu/SAPO-34 SCR catalysts upon hydrothermal aging. Catal. Today. https://doi.org/10.1016/j.cattod.2016.05.021

Ma, L., Cheng, Y., Cavataio, G., McCabe, R.W., Fu, L., Li, J., 2014. In situ DRIFTS and temperature-programmed technology study on NH3-SCR of NOx over Cu-SSZ-13 and Cu-SAPO-34 catalysts. Appl. Catal. B Environ. 156–157, 428–437. https://doi.org/10.1016/j.apcatb.2014.03.048

Martínez-Franco, R., Moliner, M., Concepcion, P., Thogersen, J.R., Corma, A., 2014. Synthesis, characterization and reactivity of high hydrothermally stable Cu-SAPO-34 materials prepared by “one-pot” processes. J. Catal. 314, 73–82. https://doi.org/10.1016/j.jcat.2014.03.018

Martínez-Franco, R., Moliner, M., Franch, C., Kustov, A., Corma, A., 2012. Rational direct synthesis methodology of very active and hydrothermally stable Cu-SAPO-34 molecular sieves for the SCR of NOx. Appl. Catal. B Environ. 127, 273–280. https://doi.org/10.1016/j.apcatb.2012.08.034

Martini, A., Borfecchia, E., Lomachenko, K.A., Pankin, I.A., Negri, C., Berlier, G., Beato, P., Falsig, H., Bordiga, S., Lamberti, C., 2017. Composition-driven Cu-speciation and reducibility in Cu-CHA zeolite catalysts: a multivariate XAS/FTIR approach to complexity. Chem. Sci. 8, 6836–6851. https://doi.org/10.1039/c7sc02266b

Mihai, O., Widyastuti, C.R., Andonova, S., Kamasamudram, K., Li, J., Joshi, S.Y., Currier, N.W., Yezerets, A., Olsson, L., 2014. The effect of Cu-loading on different reactions involved in NH3-SCR over Cu-BEA catalysts. J. Catal. 311, 170–181. https://doi.org/10.1016/j.jcat.2013.11.016

Montanari, T., Busca, G., 2008. On the mechanism of adsorption and separation of CO2 on LTA zeolites : An IR investigation. Vib. Spectrosc. 46, 45–51. https://doi.org/10.1016/j.vibspec.2007.09.001

Mrad, R., Aissat, A., Cousin, R., Courcot, D., Siffert, S., 2015. Catalysts for NOx selective catalytic reduction by hydrocarbons (HC-SCR). Appl. Catal. A Gen. 504, 542–548. https://doi.org/10.1016/j.apcata.2014.10.021

Niu, C., Shi, X., Liu, F., Liu, K., Xie, L., You, Y., He, H., 2016. High hydrothermal stability of Cu–SAPO-34 catalysts for the NH3-SCR of NOx. Chem. Eng. J. 294, 254–263. https://doi.org/10.1016/j.cej.2016.02.086

Palella, B.I., Cadoni, M., Frache, A., Pastore, H.O., Pirone, R., Russo, G., Coluccia, S., Marchese, L., 2003. On the hydrothermal stability of CuAPSO-34 microporous catalysts for N2O decomposition: A comparison with CuZSM-5. J. Catal. 217, 100–106. https://doi.org/10.1016/S0021-9517(03)00033-2

Paolucci, C., Khurana, I., Parekh, A.A., Li, S., Shih, A.J., Li, H., Di Iorio, J.R., Albarracin-caballero, J.D., Yezerets, A., Miller, J.T., Delgass, W.N., Ribeiro, F.H., Schneider, W.F., Gounder, R., 2017. Dynamic multinuclear sites formed by mobilized copper ions in NOx selective catalytic reduction. Science (80-.). 357, 898–903.

Pereda-Ayo, B., De La Torre, U., Illán-Gómez, M.J., Bueno-López, A., González-Velasco, J.R., 2014. Role of the different copper species on the activity of Cu/zeolite catalysts for SCR of NOx with NH3. Appl. Catal. B Environ. 147, 420–428. https://doi.org/10.1016/j.apcatb.2013.09.010

Petitto, C., Delahay, G., 2015. Selective catalytic reduction of NOx by NH3 on Cu-SAPO-34 catalysts: Influence of silicium content on the activity of calcined and hydrotreated samples. Chem. Eng. J. 264, 404–410. https://doi.org/10.1016/j.cej.2014.11.111

Regli, L., Bordiga, S., Zecchina, A., Bjørgen, M., Lillerud, K.P., 2005. Acidity properties of CHA-zeolites (SAPO-34 and SSZ-13): an FTIR spectroscopic study. Stud. Surf. Sci. Catal. 155, 471–479.

Rutkowska, M., Piwowarska, Z., Micek, E., Chmielarz, L., 2015. Hierarchical Fe-, Cu- and Co-Beta zeolites obtained by mesotemplate-free method. Part I: Synthesis and catalytic activity in N2O decomposition. Microporous Mesoporous Mater. 209, 54–65. https://doi.org/10.1016/j.micromeso.2014.10.011

Shen, M., Wen, H., Hao, T., Yu, T., Fan, D., Wang, J., Li, W., Wang, J., 2015. Deactivation mechanism of SO2 on Cu/SAPO-34 NH3-SCR catalysts: structure and active Cu2+. Catal. Sci. Technol. 5, 1741–1749. https://doi.org/10.1039/c4cy01129e

Shwan, S., Jansson, J., Korsgren, J., Olsson, L., Skoglundh, M., 2012. Kinetic modeling of H-BEA and Fe-BEA as NH3-SCR catalysts—Effect of hydrothermal treatment. Catal. Today 197, 24–37. https://doi.org/10.1016/j.cattod.2012.06.014

Su, W., Li, Z., Peng, Y., Li, J., 2015. Correlation of the changes in framework and active Cu sites for typical Cu/CHA Zeolite (SSZ-13 and SAPO-34) during hydrothermal aging. Phys. Chem. Chem. Phys. 17, 29142–29149. https://doi.org/10.1039/c5cp05128b

Turco, M., Bagnasco, G., Costantino, U., Marmottini, F., Montanari, T., Ramis, G., Busca, G., 2004. Production of hydrogen from oxidative steam reforming of methanol. I. Preparation and characterization of Cu/ZnO/Al2O3 catalysts from a hydrotalcite-like LDH precursor. J. Catal. 228, 43–55. https://doi.org/10.1016/j.jcat.2004.08.026

Villarreal, A., Garbarino, G., Riani, P., Finocchio, E., Bosio, B., Ramírez, J., Busca, G., 2017. Adsorption and separation of CO2 from N2-rich gas on zeolites: Na-X faujasite vs Na-mordenite. J. CO2 Util. 19, 266–275. https://doi.org/10.1016/j.jcou.2017.03.021

Wang, D., Jangjou, Y., Liu, Y., Sharma, M.K., Luo, J., Li, J., Kamasamudram, K., Epling, W.S., 2015. A comparison of hydrothermal aging effects on NH3-SCR of NOx over Cu-SSZ-13 and Cu-SAPO-34 catalysts. Appl. Catal. B Environ. 165, 438–445. https://doi.org/10.1016/j.apcatb.2014.10.020

Wang, D., Zhang, L., Kamasamudram, K., Epling, W.S., 2013. In situ-DRIFTS study of selective catalytic reduction of NOx by NH3 over Cu-exchanged SAPO-34. ACS Catal. 3, 871–881. https://doi.org/10.1021/cs300843k

Wang, D., Zhang, L., Li, J., Kamasamudram, K., Epling, W.S., 2014. NH3-SCR over Cu/SAPO-34 – Zeolite acidity and Cu structure changes as a function of Cu loading. Catal. Today 231, 64–74. https://doi.org/10.1016/j.cattod.2013.11.040

Wang, J., Fan, D., Yu, T., Wang, J., Hao, T., Hu, X., Shen, M., Li, W., 2015. Improvement of low-temperature hydrothermal stability of Cu/SAPO-34 catalysts by Cu^{2+} species. J. Catal. 322, 84–90. https://doi.org/10.1016/j.jcat.2014.11.010

Wang, J., Huang, Y., Yu, T., Zhu, S., Shen, M., Li, W., Wang, J., 2014. The migration of Cu species over Cu-SAPO-34 and its effect on NH3 oxidation at high temperature. Catal. Sci. Technol. 4, 3004–3012. https://doi.org/10.1039/c4cy00451e

Wang, J., Yu, T., Wang, X., Qi, G., Xue, J., Shen, M., Li, W., 2012. The influence of silicon on the catalytic properties of Cu/SAPO-34 for NOx reduction by ammonia-SCR. Appl. Catal. B Environ. 127, 137–147. https://doi.org/10.1016/j.apcatb.2012.08.016

Wang, L., Gaudet, J.R., Li, W., Weng, D., 2013. Migration of Cu species in Cu/SAPO-34 during hydrothermal aging. J. Catal. 306, 68–77. https://doi.org/10.1016/j.jcat.2013.06.010

Westermann, A., Azambre, B., Bacariza, M.C., Grac, I., Ribeiro, M.F., Lopes, J.M., 2017. The promoting effect of Ce in the CO2 methanation performances on NiUSY zeolite : A FTIR In Situ/Operando study. Catal. Today 283, 74–81. https://doi.org/10.1016/j.cattod.2016.02.031

Westermann, A., Azambre, B., Bacariza, M.C., Grac, I., Ribeiro, M.F., Lopes, J.M., Henriques, C., 2015. Insight into CO2 methanation mechanism over NiUSY zeolites : An operando IR study. Appl. Catal. B Environ. 174–175, 120–125. https://doi.org/10.1016/j.apcatb.2015.02.026

Wilken, N., Wijayanti, K., Kamasamudram, K., Currier, N.W., Vedaiyan, R., Yezerets, A., Olsson, L., 2012. Mechanistic investigation of hydrothermal aging of Cu-Beta for ammonia SCR. Appl. Catal. B Environ. 111–112, 58–66. https://doi.org/10.1016/j.apcatb.2011.09.018

Xiang, X., Yang, M., Gao, B., Qiao, Y., Tian, P., Xu, S., Liu, Z., 2016. Direct Cu2+ ion-exchanged into as-synthesized SAPO-34 and its catalytic application in the selective catalytic reduction of NO with NH3. RSC Adv. 6, 12544–12552. https://doi.org/10.1039/c5ra22868a

Yu, T., Hao, T., Fan, D., Wang, J., Shen, M., Li, W., 2014. Recent NH3-SCR Mechanism Research over Cu/SAPO-34 Catalyst. J. Phys. Chem. C 118, 6565–6575.

Yu, T., Wang, J., Shen, M., Li, W., 2013. NH3-SCR over Cu/SAPO-34 catalysts with various acid contents and low Cu loading. Catal. Sci. Technol. 3, 3234–3241. https://doi.org/10.1039/C3CY00453H

Yu, T., Wang, J., Shen, M., Wang, J., Li, W., 2015. The influence of CO2 and H2O on selective catalytic reduction of NO by NH3 over Cu/SAPO-34 catalyst. Chem. Eng. J. 264, 845–855. https://doi.org/10.1016/j.cej.2014.12.017

Zabilskiy, M., Djinović, P., Erjavec, B., Dražić, G., Pintar, A., 2015. Small CuO clusters on CeO2 nanospheres as active species for catalytic N2O decomposition. Appl. Catal. B Environ. 163, 113–122. https://doi.org/10.1016/j.apcatb.2014.07.057

Influence of CO_2 and H_2O co-feeding in the NO_x abatement by SCR over an efficient Cu-CHA catalyst

Marina Cortés-Reyes, M. Ángeles Larrubia, Concepción Herrera, Luis J. Alemany*

Departamento de Ingeniería Química, Facultad de Ciencias, Campus de Teatinos, Universidad de Málaga, Málaga, E-29071, Spain

**Corresponding author. Tel. and Fax: +34 952131919; e-mail address: luijo@uma.es*

Abstract

Cu-SAPO-34 materials with 2wt% of copper synthesized in one pot with all the copper inside the framework are hydrothermally stable. Copper oxide species were not detected by XRD after thermal and hydrothermal aging at 750 ºC. CO_2 and H_2O molecules are retained on Cu-SAPO catalyst and are related to CO_2 adsorption aided by water involving the Cu-species. Copper species coordination is modified by the reaction atmosphere and the species are directly involved in the SCR-process. A decrease in the ammonia storage capacity in the presence of water has been justified due to the cooperative competition between the ammonia and water adsorption and/or CO_2 carbonation over the same sites. Higher coordinated Cu species localized inside of CHA-framework, up to a loading close to 4% with this methodology, are highly efficient in the removal of NO_x by reaction with ammonia, in the presence of oxygen, water (1.5%) and CO_2 (0.3%) as reaction atmosphere. The SCR mechanism is essentially the same as in dry conditions because the Cu^{2+}/Cu^{+} ions, in equilibrium with H_2O+CO_2, are the active species in the SCR-reaction. Hydrated-carbonated Cu(II) and Cu(I) species are associated with the redox-chemistry of NO_x abatement as responsible for the improvement in the standard SCR; favoring the hindering of ammonia oxidation and nitrate decomposition. In the SCR temperature range, the conversion values registered for this catalyst are higher than 80% with total selectivity to N_2.

Keywords: Cu-CHA catalyst, copper species, hydrothermal stability, SCR-DeNO$_x$, real conditions, CO_2 and H_2O co-adsorption

1. Introduction

Nowadays, the obtaining of zero emission at the outlet gas of a diesel engine is expected to be achieved by the use of coupled technologies NSR-SCR (NO_x Storage and Reduction – Selective Catalytic Reduction) (Bonzi et al., 2010; Can et al., 2015; De La Torre et al., 2016b; Lindholm et al., 2010). Regarding the SCR catalytic bed, zeolitic materials are presented as more suitable NH_3-traps due to their acidity and structure (Colombo et al., 2012a), their high performance at low temperature conditions and their efficiency at high space velocities. Lots of zeolites have been proposed, such as ZSM5 or BETA, with completely different characteristics, framework types or Si/Al ratios, which are important factors for the catalytic properties of the materials (De La Torre et al., 2012; Heo et al., 2011; Kim et al., 2012; Mihai et al., 2014; Mrad et al., 2015). Recently, zeolites with small pore diameter such as chabazite (3.8Å) have been proposed to improve hydrothermal stability with regard to large pore zeolites (Blakeman et al., 2014; Kim et al., 2014; Martínez-Franco et al., 2012), since the pore size is smaller than the diameter of $Al(OH)_3$ and inhibits the dealuminitation process (Blakeman et al., 2014; Leistner and Olsson, 2015). Significant numbers of recent works compare this type of structure with other materials and ensure that SAPO-34 acts effectively in the SCR temperature range and has a better resistance to thermal aging and hydrothermal stability than others, such as SSZ-13, for example (Ma et al., 2014; D. Wang et al., 2015). In addition, a metal is required in the formulation in order to effectively act on the selective catalytic reduction. There are several works in which the differences between the use of iron or copper are detailed (Cheng and Bi, 2014; Colombo et al., 2010). Fe-zeolites usually have less ammonia storage capacity than Cu-zeolites and the latter being more active in the ammonia oxidation process and presenting higher SCR activity at low temperatures, as well as high efficiency in the N_2O decomposition process (Chen et al., 2016; Colombo et al., 2012b; Rutkowska et al., 2015). Therefore, Cu-SAPO-34 can be considered as a promising material for this technology. The content of metal is another key point since a high metal content could lead to extra-framework metal oxide clusters that are active for parallel reactions such as ammonia oxidation or nitrate formation (Brandenberger et al., 2008; De La Torre et al., 2012; Mihai et al., 2014; Shwan et al., 2012). The synthesis method also influences the catalytic activity and the location of the active species. For that reason, in a previous work (Cortés-Reyes et al., 2017) the one-pot synthesis of Cu-SAPO-34 materials with all the copper inside the framework has been widely studied.

The hydrothermal stability of the zeolite and its behaviour in the presence of water are two main concerns in the use of these materials as SCR catalysts. In addition to the beneficial effect of the small pore zeolites on hydrothermal stability, as has been demonstrated in the bibliography, copper species migrate from the external surface into the micropores during hydrothermal treatment at high temperatures (L. Wang et al., 2013), improving the redox ability of the aged Cu/SAPO-34 zeolite and maintaining its acidic properties (Gao et al., 2015; Su et al., 2015). The migration of surface clusters into the cavities also suppresses competitive ammonia oxidation (Liu et al., 2016). During thermal aging the copper ions could be stronger bound as if structural Cu^{2+} were present (Palella et al., 2003). However, several authors have exposed these materials to extreme conditions and have not always obtained good results. The exposure of a Cu-SAPO-34 synthesized in one-pot to a stream with 80% of humidity at 70 ºC produced the collapse of the structure; however, this effect decreased with an increase in copper content, and Cu^{2+} ions seem to be the active species and structure protective agents (J. Wang et al., 2015). *K. Leistner et al*. (Leistner and Olsson, 2015) have also observed similar effects when a Cu/SAPO-34 synthesized by exchanged was exposed to a feed containing water vapor at temperatures below 100 ºC. Nevertheless, the structural changes in the presence of water and after hydrothermal aging are still not clear for catalysts synthesized in one pot with the copper inside.

The study of the SCR reaction in the presence of water and CO_2 simultaneously is also relevant because of the presence of these compounds in exhaust gas. *T. Yu et al.* (Yu et al., 2015) investigated the influence of water and CO_2 in the SCR reaction over a Cu/SAPO-34 synthesized by solid state ion exchange, and observed that the CO_2 did not present a high impact on the conversion, whereas the water presence improved the acidity of Brönsted acid sites and the reducibility of the Cu^{2+} species and, therefore, the SCR activity. The isolated copper species can be modified in the presence of water and converted into a hydrated copper species, which is the active site (Bates et al., 2014). Other authors have shown that Cu^{2+} are the active species via ammonia solvated intermediate modifying the redox-cycle during the process (Gao et al., 2017; Paolucci et al., 2017). However, the influence of the combination of water and CO_2 in the SCR activity and the co-side reactions together with the structural changes and the active metal species have not previously been considered in detail.

Several authors indicate that CO_2 does not influence the SCR activity, whereas the presence of water inhibits the co-side reactions; nevertheless, the effects of the combination of water and CO_2, real conditions, on the hydrothermal stability, the metal species and the SCR performance have not been evaluated. Therefore, the influence of the combination of water and CO_2 remains unclear in the literature and will be addressed in this work, using a Cu-SAPO-34 material that has been directly synthesized with limited extra-framework copper ions. The hydrothermal stability, the active species and their location and the SCR efficiency in water and CO_2 environment are going to be studied.

2. Experimental

2.1. Materials preparation and characterization

SAPO-34 was synthesized by ultrasound assisted hydrothermal method, using the molar gel composition: 2 DEA: 0.6 SiO_2: 1 Al_2O_3: 0.8 P_2O_5: 50 H_2O, keeping the mixtures autoclaved at 200 ºC during 4h. After that, the solid product was filtered and washed with distilled water and dried at 110 ºC overnight. Finally, it was calcined at 550 ºC in air for 5h. The detailed procedure is reported in previous works (Cortés-Reyes et al., 2017, 2016). Copper (2wt%, expressed as copper metal) was incorporated during the synthesis process, by complexation of copper and TEPA (tetraethylenepentamine, Sigma Aldrich) in a molar ratio 1:1.

The catalysts were characterized by different techniques. X-ray Powder Diffraction data were recorded with an X'Pert MPD PRO diffractometer (PANalytical) using Cu Kα1 radiation (λ=1.54059 Å) and a Ge(111) primary monochromator. The X-ray tube worked at 45 kV and 35 mA. The measurements were registered from 5º to 80º (2θ). The composition of the samples was analyzed with the XGT-5000WR Fluorescence spectrometer by X-ray dispersive energy. N_2 adsorption-desorption isotherms were obtained at 77K using a Micromeritics ASAP 2020 Analyzer. Before the analysis, the samples were outgassed in vacuum ($1\cdot10^{-3}$ Pa) for 5h at 453K. UV-Vis Diffuse Reflectance spectra were registered with a T92+UV Spectrophotometer (PG Instruments), equipped with conventional integrating sphere. X-ray Photoelectron Spectra were recorded by using a Physical Electronic 5701 equipped with a PHI 10-360 analyzer using the MgKα X-ray source. The values of binding energy (BE) were referred to the C1s peak (284.8 eV) from the adventitious carbon. All deconvolutions of experimental curves were done with Gaussian-Lorenzian line fitting of varying proportions (60-80%). Adequate and short times of exposure were used in order to diminish the reduction of the copper.

2.2.Hydrothermal stability

The thermal aging and hydrothermal stability were performed by non-isothermal and isothermal protocol in water and water-free environments. The TG-DTA and mass signals were recorded with the SDT Q600 thermobalance from T.A. Instrument connected to a Pfeiffer Prima^{TM} Quadrupole Mass Spectrometer QMS 200. The runs were carried out by steaming 20 mg of the samples with 1% of water in Helium, heating the sample from r.T. to 750 ºC at 10K·min^{-1}, keeping at this temperature for 5h. The analysis of the zeolite structure was studied by XRD Rietveld refinement.

2.3.Catalytic activity

Catalytic tests were performed in a fix bed reactor consisting of a quartz tube, loaded with 60 mg of powder catalyst (100-125 µm) and working without outer diffusional problems. A total flow of 100 cm^{3}min^{-1} (at 1 atm and 0 ºC) was used in all the experiments. The reactor was directly connected to a mass spectrometer (QMS 200, *Pfeiffer Vacuum Prisma*^{TM}) and a micro-gas chromatograph (3000A, *Agilent*) in a parallel arrangement to analyze the reaction products.

Ammonia trap capacity was tested by isothermal ammonia adsorption experiments at different temperatures (150-450 ºC), feeding 750ppm of NH_3 in He for two hours, and then a Helium purge of 90 min was performed in order to remove the physisorbed ammonia. Finally, the sample was heated up to 500 ºC at 15 K·min^{-1}. The catalytic activity for the standard SCR process was studied at different temperatures (150-500 ºC), exposing the sample to a flow that was composed of 750ppm NH_3, 750ppm NO and 3%O_2. To individualize the processes, ammonia oxidation was also studied, introducing a stream of 750ppm of NH_3 and 3% of O_2. All these processes were also performed in 1.5% H_2O+0.3% CO_2 atmosphere.

2.4. CO_2 adsorption study

In order to study the influence of the presence of water in the CO_2 adsorption, TG-MS experiments were carried out in a thermobalance, using 10mg of the sample and 100 ml·min^{-1} of total flow. CO_2 was fed into the chamber in the presence and absence of 1% of H_2O at 200ºC until the saturation of the surface. The product distribution was registered by the QMS

200, *Pfeiffer*. In addition, the same experiments were performed over the self-supported disk of the sample held in a cell connected to a vacuum system that allow the analysis by FTIR. Over the activated surface at 500ºC, 5 torr of CO_2 were adsorbed at 200ºC in dry conditions or over the surface previously hydrated with 3 torr of water. Spectra were recorded at different temperatures.

3. Results and Discussion

The characterization of this type of material has been well detailed in a previous work (Cortés-Reyes et al., 2017). Nevertheless, some relevant data are here explained. The composition of the catalysts was analyzed by XRF. The resulting (Al+P)/Si and Cu/Si ratio of the materials are 8 and 0.5, respectively, and in consequence Si/Al and Cu/Al ratio are 0.2 and 0.1, respectively. These values and the content of each element are quite similar to the theoretical amount used in the synthesis gel composition. The low silica content and copper concentration are in line with the data reported for other authors in the study of SAPO-34 based materials (Martínez-Franco et al., 2014)(Yu et al., 2013).The textural properties for these materials are shown in Table 1. Superficial area and micropore volume values are similar to those reported in the bibliography, in spite of the different copper concentrations, P/Al ratio and the synthesized method (Fan et al., 2013; Leistner and Olsson, 2015; Niu et al., 2016; Shen et al., 2015; Xiang et al., 2016; Yu et al., 2015) and closer to 560 $m^2 \cdot g_{cat}^{-1}$.

Table 1. Textural properties of SAPO-34 and 2Cu-SAPO-34.

Catalyst	**S_{BET} ($m^2 \cdot g^{-1}$)**	**V_μ ($cm^3 \cdot g^{-1}$)**	**V_μ /V_p (%)**
SAPO-34	559	0.24	82
2Cu-SAPO-34	556	0.22	79

These materials are mainly microporous and the incorporation of copper did not destroy the structure. In fact, the micropore/total pore volume ratio for SAPO-34 is 83%, and this value only decreases to 79% with the copper incorporation, maintaining the micropore volume close to 0.22 $cm^3 \cdot g_{cat}^{-1}$.

The species location and distribution for 2Cu-SAPO-34 were analyzed by UV-Vis-DR and XPS. The UV-Vis-DR spectra recorded for both catalysts are displayed in Figure 1 and the profiles are similar to those previously reported (Cortés-Reyes et al., 2017, 2016). For SAPO-

34, a weak peak was detected around 255 nm and as other authors have described (Dang et al., 2009; L. Wang et al., 2013) is associated with the charge transfer (CT) band of the zeolite $(O^{2-} \rightarrow Al^{3+})$ and no additional signals were registered in the whole visible range.

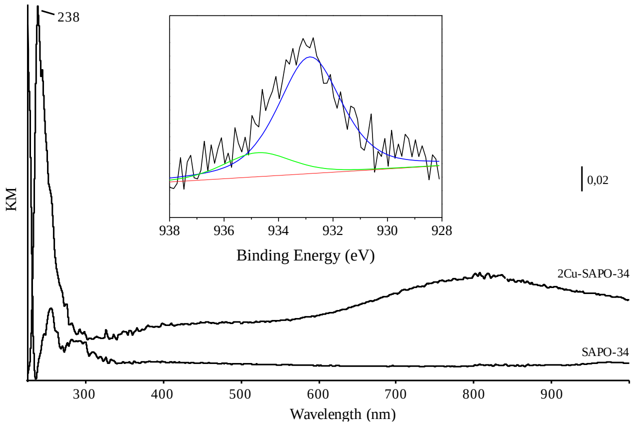

Figure 1. UV-Vis-DR spectra of SAPO-34 and 2Cu-SAPO-34 and XPS of Cu2p region of 2Cu-SAPO-34 (inset).

For 2Cu-SAPO-34, the UV-Vis-DR spectrum is completely different and several intense signals appeared. The most energetic signal was observed at 238 nm and was related to $O^{2-} \rightarrow Cu^{2+}$ ligand to metal charge transfer transition of isolated Cu^{2+} species in agreement with *M. Turco et al.* (Turco et al., 2004). In addition, the broad band centered at 800 nm was assigned to electron d-d transitions of Cu^{2+} ions in distorted octahedral symmetry (Leistner and Olsson, 2015; Turco et al., 2004; L. Wang et al., 2013). Signals related to di-nuclear copper species were barely detected around 425nm. Only Cu^{2+} species can be detected by UV-Vis-DR spectroscopy.

XPS confirms the presence of Cu^{+} species besides Cu^{2+} species. The deconvolution of the Cu2p signal for the fresh catalyst at room temperature is also displayed inside Figure 1. In consonance with other authors (Andonova et al., 2014; Biesinger et al., 2010; Cao et al., 2015; Niu et al., 2016; Pereda-Ayo et al., 2014; L. Wang et al., 2013) that have delved into the XPS analysis of copper, a signal below 933 eV (932.8 eV) and other above (934.8 eV) were observed, as well as the satellite around 943 eV (not shown), necessary to confirm the Cu^{2+} presence. The first represents the 65% of the total amount of copper and, taking into account the Auger parameter, was associated with Cu^{+} species. The latter, 35%, corresponds to isolated Cu^{2+} species. It is noteworthy that these values do not have to coincide with the Cu^{+}/Cu^{2+} ratio under the reaction atmosphere, but as reported by *A. Martini et al.* (Martini et al., 2017) both species are involved in the process. On the catalyst surface, a combination of Cu^{+} and Cu^{2+} oxidized-species was observed, with a higher population of Cu^{+} species. Although the amount of Cu^{+} species could be overestimated due to the fact that is a superficial technique and a partial photoreduction could take place, despite working with short exposure times. However, the values are similar to those reported by other authors (Chen et al., 2014; Wilken et al., 2012) and in consonance with previous works (Cortés-Reyes et al., 2017) where the easy reduction of Cu^{2+} to Cu^{+} was demonstrated.

The hydrothermal stability of the samples analyzed by TG-MS experiments indicated that the evolution of the weight profile and the specific heat flow with the time and the temperature for 2Cu-SAPO-34 are identical regardless of the presence of water in the atmosphere. Moreover, no severe changes in the sample were detected as consequence of the thermal aging. However, the XRD patterns and the unit cell characteristic obtained by Rietveld refinement for the fresh 2Cu-SAPO-34 and after the hydrothermal aging, which are displayed in Figure 2, revealed a slight modification of the structure. A structurally apparent modification was not observed in the diffractogram when CO_2 was present.

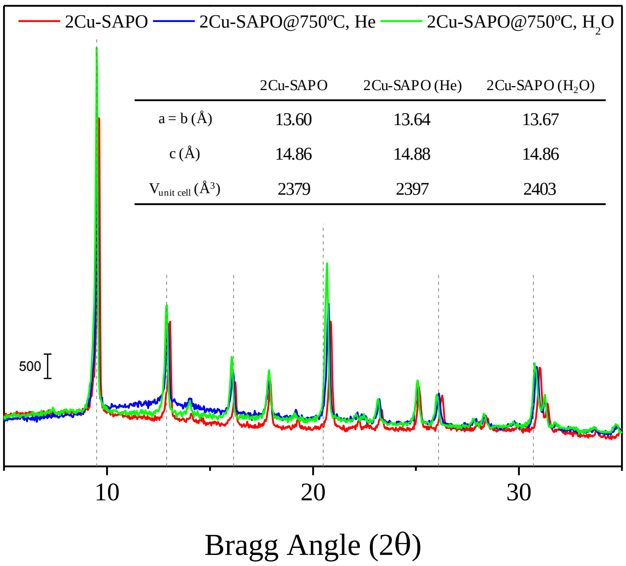

	2Cu-SAPO	2Cu-SAPO (He)	2Cu-SAPO (H_2O)
a = b (Å)	13.60	13.64	13.67
c (Å)	14.86	14.88	14.86
$V_{unit\ cell}$ (Å^3)	2379	2397	2403

Figure 2. X-ray diffraction patterns of 2Cu- SAPO-34 (fresh and after thermal aging in He and in H_2O) and unit cell values (inset table).

In all cases, the XRD patterns showed the diffraction lines associated with chabazite (CHA) structure (JCPDS 01-087-1527) with 2θ signals at 9.4, 12.9, 16.15, 20.5, 26.1 and 30.5º, representative of SAPO-34 samples (Álvaro-Muñoz et al., 2012; Cui et al., 2013; Petitto and Delahay, 2015), with crystal sizes of around 1-5 µm. For the fresh 2Cu-SAPO-34, peaks related to copper oxide were not detected around 35.4 and 38º, as other authors have observed (Gao et al., 2015; D. Wang et al., 2014; Zabilskiy et al., 2015), when the materials are synthesized by ion-exchange method or wet impregnation. The comparison between the 2Cu-SAPO-34 and the wet aged materials did not show a significant difference in the structure and it could even seem that the hydrothermal aging slightly increases the crystallinity. No other copper phases, such as Cu, Cu_2O or CuO, were detected, in line with that reported by *D. Wang et al.* (D. Wang et al., 2015) for a Cu-SAPO-34 synthesized by ion-exchange of a commercial material with 4% of copper or *J. Wang et al.* (Wang et al., 2012) with the same procedure but a lower copper percentage (1%). Nevertheless, as can be observed in the inserted table, the data obtained by Rietveld refinement pointed out an almost insignificant increase in the unit cell volume of 0.8 and 1% for dry and wet conditions, respectively, caused by the hydrothermal treatment. Regarding the distances, the parameter “c” did not suffer any modification, whereas “a” and “b” distances increased, indicating that the cell widens. Other authors have also observed a lattice expansion of the SAPO-34 support after the hydrothermal aging when a 0.9% of copper was incorporated by ion-exchange (L. Wang et al., 2013). Although it is possible to find some work (Cao et al., 2015) that indicates the significantly decrease of crystallinity over a Cu-SAPO-34 synthesized by wetness impregnation, it is generally accepted that the ion exchange method (Duan et al., 2015; Fan et al., 2013; J. Wang et al., 2014) or even the one-pot synthesis with different precursors and protocols (Gao et al., 2015) produce materials with high hydrothermal stability and the copper is well dispersed or may have migrated into the SAPO-34 cavity, next to 8-membered rings. Therefore, hydrated copper in octahedral position and the structure are minimally affected by hydrothermal aging.

In order to study the influence of the water and CO_2 presence in the ammonia adsorption capacity, NH_3-TPD of the different samples activated during 1h at 500ºC in reaction environment were performed in He and in H_2O+CO_2 atmospheres, adsorbing 750 ppm of NH_3 up to saturation (around 2 hours) at several temperatures (150-450 ºC, 100 ºC steps) of the operation range. In all cases, an hour is needed to obtain the completely saturation of the catalyst; however, the breakthrough time and the adsorption rate depend on the temperature and the reaction atmosphere. In dry conditions, an increase in the temperature produces an increment in the adsorption rate and a decrease in the breakthrough time. Nevertheless, in water and CO_2 environment higher values of the breakthrough time were detected, whereas the saturation was faster, increasing the rate with respect to the experiments in Helium.

Values of net adsorbed NH_3 (mmol $NH_3.g_{cat}^{-1}$) calculated subtracting the ammonia desorbed in the purge are shown in Table 2 and are similar to the previously reported (Duan et al., 2015).

Table 2. NH_3 adsorption values (mmol·g_{cat}^{-1}) of NH_3-TPD experiments.

Temperature (ºC)	150	250	350	450
SAPO-34 (He)	0.87	0.55	0.20	0.16
SAPO-34 (H_2O+CO_2)	0.82	0.51	0.18	0.14
2Cu-SAPO-34 (He)	0.87	0.53	0.18	0.11
2Cu-SAPO-34 (H_2O+CO_2)	0.76	0.43	0.11	0.05

As general trend, it is possible to assume that the ammonia adsorption capacity decreases with the increase of temperature, as expected, independently of the copper presence or the reaction atmosphere. When copper is present in the structure, the retention was slightly lower than SAPO-34, indicating that the SAPO-34 is the main responsible for the overall ammonia adsorption capacity. The decrease in the acid sites of SAPO-34 with the loading of copper can be justified due to the substitution of the proton (-Si-OH-Al-) of the support by Cu^{2+} species (Duan et al., 2015; Wang et al., 2012). The presence of water and CO_2 in the reaction atmosphere caused a decrease in the ammonia adsorption capacity, being more evident for 2Cu-SAPO-34. Some authors (Yu et al., 2015) have observed an increase in the adsorbed NH_3 contents by an increment in the acid density, whereas in general a decrease in the ammonia storage in the presence of water has been justified due to the cooperative competition between the ammonia and water adsorption and/or CO_2 carbonation over the same sites (Leistner and Olsson, 2015). The data of the reduction of the ammonia storage capacity due to the presence of water and CO_2, expressed as percentage, are represented in Figure 3.

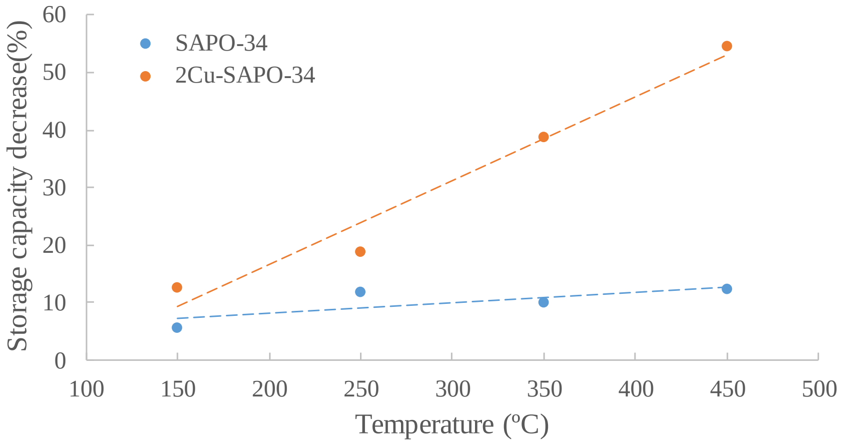

Figure 3. Ammonia storage capacity decrease percentage in the presence of 1.5%H_2O and 0.3% CO_2 in relation to dry conditions.

These data indicated that the adsorption capacity seems not to be further affected by temperature for the SAPO-34 material, since the slope of the fitted data according to temperature remains close to $0.1.10^{-3}$. Nevertheless, the slope registered for 2Cu-SAPO-34 increased ten times with respect to Cu-free catalyst. This fact is associated with the impact of H_2O+CO_2 combination on the NH_3 adsorption, related to overall acidity behavior of copper species. Therefore, the reduction of acid sites corresponds to the partial occupancy of sites by some kind of hydro-carbonation of Cu species. The latter is responsible for the expansion of the NH_3-breakthrough-time and the faster saturation rate. Even though the ammonia storage capacity can decrease in the presence of water and CO_2, because of the modification of the acid centers in agreement with other authors (Busca et al., 1998; Su et al., 2015; Wang et al., 2012; Yu et al., 2015), a high capacity value was kept, making its use as ammonia trap possible.

The SCR activity was studied in a flow reactor, feeding 750ppm of NH_3, 750ppm of NO and 3% of O_2 in He (dry conditions) or 1.5% of H_2O and 0.3% of CO_2 (mix-conditions). In Figure 4, the SCR activity parameters, such as ammonia and NO conversion and N_2, N_2O and NO_2 selectivity, are displayed in the studied temperature range (150-500 ºC) for the Cu-free and Cu-SAPO-34 catalysts. Regarding the SAPO-34 behavior in dry conditions, the NO-conversion is low registering the maximum value at 250 ºC close to 30%. Above this temperature, the NO conversion decreased below zero, pointing out that NO production occurs. However, the NH_3 conversion increased with the temperature up to the total conversion above 300 ºC. So, the ammonia reacts with the available oxygen, via ammonia oxidation in gas phase, producing not only nitrogen, but also N_2O, NO and NO_2. It should also be noted that high levels of N_2O formation are measured around 250 ºC and its production is related to surface nitrate decomposition. This agrees with those data reported by *T. Yu et al.* (Yu et al., 2015) for a hydrothermally synthesized SAPO-34 where they observed low NO conversion values, ammonia oxidation from 300 ºC and N_2O generation with a maximum at 320 ºC. In SCR-mix conditions (i.e. H_2O+CO_2), NO and NH_3 conversion values and selectivity trends are almost identical to dry conditions, indicating that the H_2O+CO_2 combination does not affect the already low SCR activity for SAPO-34.

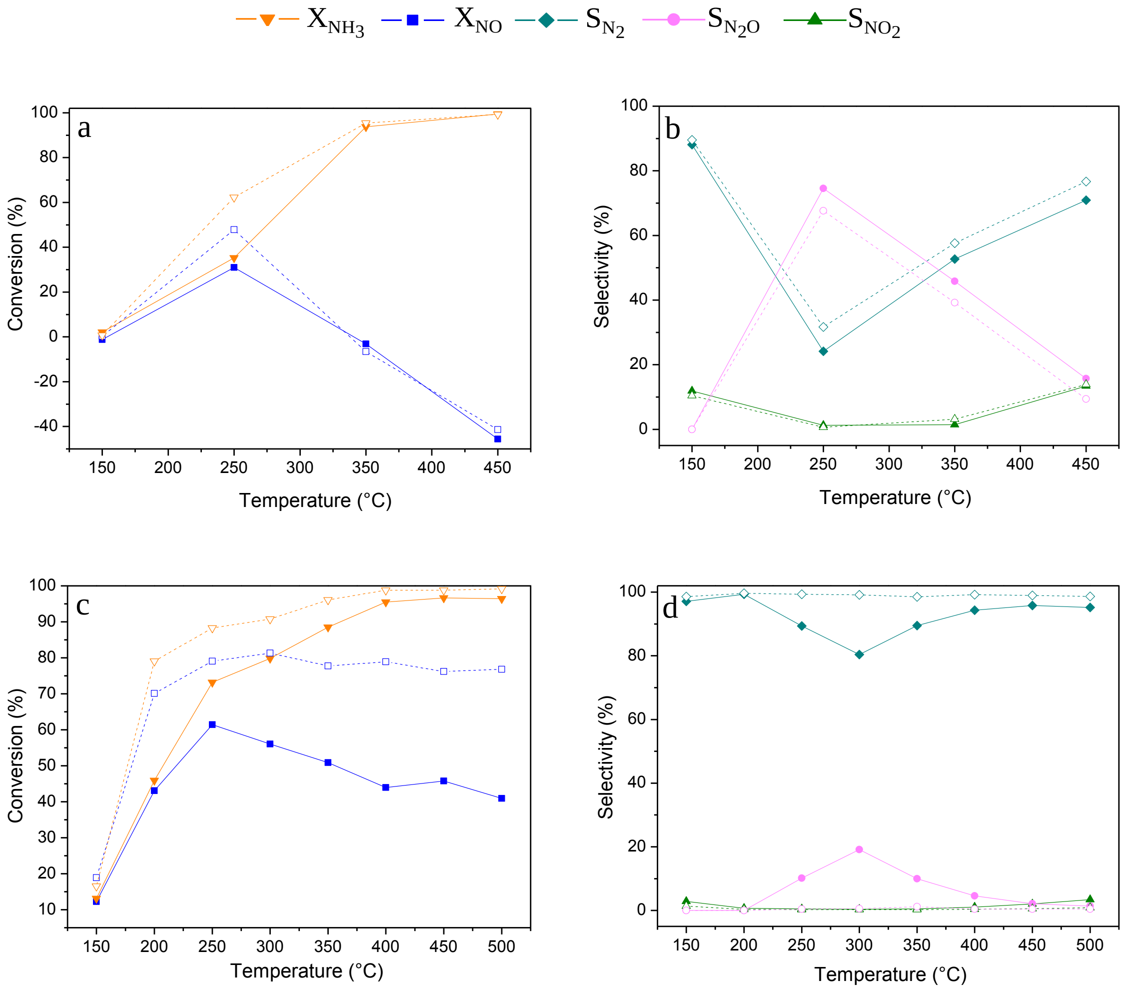

Figure 4. SCR activity parameters (conversion and selectivity) for SAPO-34 (a, b) and 2Cu-SAPO-34 (c, d) in He (solid lines) and in H_2O + CO_2 atmosphere (dotted lines)

For 2Cu-SAPO-34, the profiles of conversion and selectivity in dry conditions are displayed in Figures 4c and 4d and indicated that there are several reactions taking place. At low temperatures (up to 200 ºC), the conversion of NH_3 and NO was stoichiometric producing nitrogen and water, which means that the standard SCR occurs. In the SCR temperature range, between 200 and 400 ºC, and up to 500 ºC, the NH_3 conversion was higher than NO conversion, indicating another via of ammonia consumption without NO intervention, which is the ammonia oxidation. *D. Wang et al.* (D. Wang et al., 2013) also observed the NH_3 oxidation together with a decrease in the NO conversion at temperature higher than 200 ºC with a copper exchange commercial SAPO-34. Furthermore, there was a significant N_2O formation with a maximum at 300 ºC associated with the direct nitrate decomposition, which occurs in this temperature range. By in situ-FTIR analysis (Cortés-Reyes et al., 2016) and dynamic pulse experiments, the adsorption of NO over this catalyst has been carried out in dry conditions. For this catalyst, nitrate formation was observed and at temperature values higher than 300ºC, their decomposition with N_2O formation. These experiments are in accordance with *T. Yu et al.* (Yu et al., 2014) who reported that the decomposition of nitrates produces N_2O, since it is the most probably side reaction.

From the activity data, it has been confirmed that the presence of H_2O and CO_2 in the reaction atmosphere provoked a significant modification in the processes that take place. At low SCR-temperature range (<200 ºC) the conversions of NO and NH_3 were almost identical with total nitrogen production (Fig. 4c and 4d). So, the standard SCR is the main reaction with a NO and NH_3 conversion of 75% and a complete selectivity to N_2. In the temperature range between 200 and 500 ºC, the NH_3 conversion remained higher than that of NO, pointing out that besides the standard SCR, the ammonia oxidation occurs in minor extent that registered in dry conditions; both lead to N_2 selective production. It is noteworthy that N_2O was not detected in the temperature range, meaning that the side-reactions with undesired compounds production are also hindered, enhancing the SCR activity due to the inhibition of N_2O production (Busca et al., 1998). Other authors (Yu et al., 2015) indicated that CO_2 presence in the feeding apparently did not influence the SCR activity for a Cu-SAPO-34 prepared in two steps at low Cu loading (<1%) incorporated by ion-exchanged, whereas the H_2O addition improved the NH_3-SCR activity and the NO_2 and N_2O selectivity values decreased. *U. De La Torre et al.* (De La Torre et al., 2016a) have observed an increase in the N_2O production at intermediate temperatures after the hydrothermal aging and have related it to the partial loss of the acidity and the micropore volume of the catalysts. On the contrary, in the presence of water and CO_2, despite the variation of the acidity, the structure was not modified and the N_2O production was completely hindered, thence, the inhibition of a reaction responsible for the N_2O formation takes place, which could be related to the chemical environment of the copper species being changed. H_2O and CO_2 combination should be responsible for the improved NH_3-SCR performance over the model 2Cu-SAPO-34 catalyst, due to the inhibition of side reaction such as the nitrate decomposition route and ammonia oxidation.

In order to confirm the beneficial effect of H_2O+CO_2 combination on the SCR-DeNO$_x$, ammonia oxidation experiments were carried out and compared in dry and wet conditions, both of them were also studied in the same reactor, feeding 750 ppm of NH_3 + 3% of O_2, being the results shown in Figure 5.

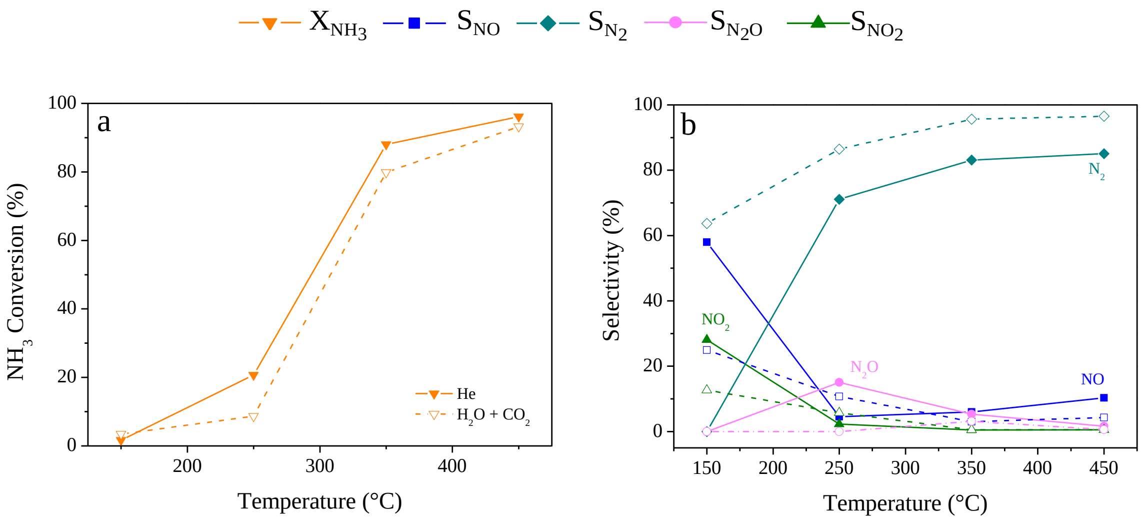

Figure 5. NH_3 oxidation conversion (a) and selectivity (b) values vs temperature in He (solid lines) and in H_2O+CO_2 (dotted lines) atmospheres for 2Cu-SAPO-34.

The NH_3 conversion increased with the temperature independently of the atmosphere, with values higher than 90% at temperatures above 300 ºC in dry conditions. At low temperatures, the conversion values were insignificant and, therefore, the selectivity values cannot be considered as representative, since the concentrations of the products were minimal. Around 250 ºC, there was a slight formation of N_2O, which can contribute to the N_2O production detected in the SCR experiments. However, the increase of the temperature did not produce a higher amount of this component, and the maximum detected in the previous experiments has to involve another process.

The presence of water and CO_2 not only inhibits the ammonia oxidation, but also increases the nitrogen selectivity, in agreement with the observed in the SCR conditions. In addition, there was no production of N_2O in the whole temperature range because the centers responsible for nitrate formation are blocked as has been explained above. It is noteworthy that several authors have detected NO as the main product of the oxidation, because of its formation in CuO species (J. Wang et al., 2014), which are not present in this one-pot synthesized material. Regarding the inhibition of ammonia oxidation in presence of water and CO_2 in this material, Cu^+ species would be stabilized in Cu^+-hydrated-carbonated form and, probably, these species inhibit ammonia oxidation. These data are in accordance with that reported by other authors (D. Wang et al., 2014; J. Wang et al., 2014; Yu et al., 2015), in which the Cu_xO_y clusters or Cu^+ species responsible for the ammonia oxidation are reduced as consequence of the water interaction.

In order to study the dependence of the water presence in the carbonation of the materials, TG-MS isothermal experiments were carried out adsorbing CO_2 in the presence and absence of water until the saturation of the sample. It should be noticed that CO_2 was not adsorbed onto the catalyst in the absence of water, indicating that in dry conditions, the catalyst is not carbonated, regardless of the copper species. The TG profile after the water adsorption is displayed in Figure 6 and presents a typical adsorption curve, which after 100 min reached a weight gain of about 0.35% of its initial weight in consonance with the signals obtained by mass spectrometry.

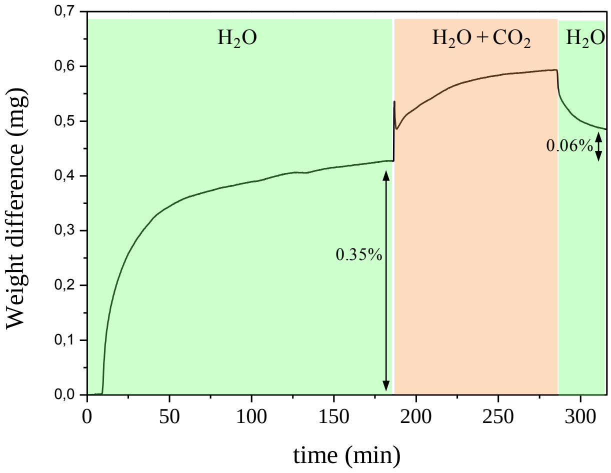

Figure 6. Weight difference profile along the time for water and CO_2 adsorption over 2Cu-SAPO-34 registered by TGA at 200 ºC.

In Figure 7, the CO_2 profile during the adsorption is represented for both conditions. In water environment (wet), the consumption of CO_2 was detected due to the CO_2 adsorption over the previously hydrated sample; different from the dry adsorption that did not produce a net CO_2 adsorption. It is noteworthy that the coadsorption at 200ºC of both compounds, H_2O and CO_2, produced a storage of around 40 µmol of $CO_2 \cdot g_{cat}^{-1}$, when the catalyst was previously hydrated with 75 µmol of $H_2O.g_{cat}^{-1}$.

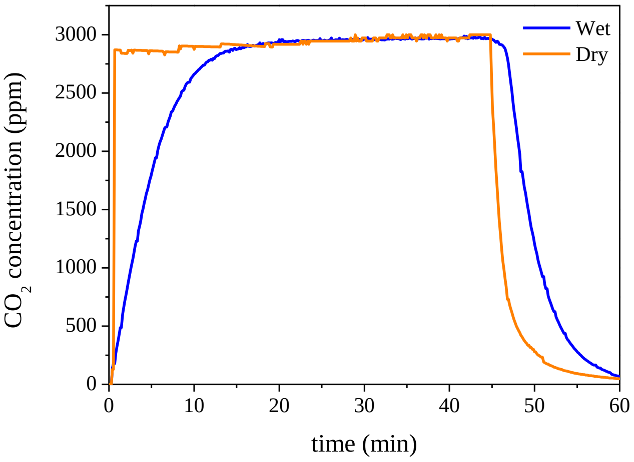

Figure 7. CO_2 profile during the adsorption in the presence of water (wet) and He (dry).

A comprehensive explanation about how CO_2 and H_2O molecules are retained on Cu-SAPO-34 catalyst should be related to CO_2 adsorption aided by water involving Cu-species. Copper species (in oxidation state (I) and (II)) are stabilized and chemically modified in this environment and they are directly involved in the SCR-process, through the carbonated-hydrated species, produced in these conditions.

The modification of the species due to the presence of water and CO_2 was also analyzed by FTIR and the spectra of the adsorption of CO_2, water and H_2O+CO_2 at 200 ºC with the subtraction of the activated sample are represented in Figure 8; prior to the adsorption, the surface was activated at 500ºC for 2h under vacuum to completely clean the surface.

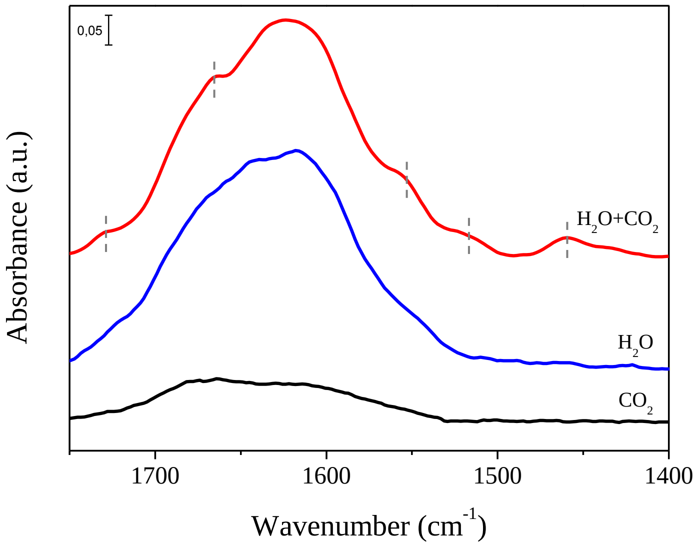

Figure 8. FTIR spectra after adsorption and outgassing at 200 ºC of CO_2, water and CO_2 and water over 2Cu-SAPO-34.

The adsorption of CO_2 barely produced the modification of the spectra, in consonance with the TG-MS experiments in which the carbon dioxide was not adsorbed. For the water adsorption, the main signal was broad and detected in the region between 1800 and 1500 cm^{-1}, with a maximum at 1620 cm^{-1}, due to the bending mode of water adsorbed onto the surface of the catalyst (Bordiga et al., 2005). The hydrophilic character of SAPO-34 materials is already known (Regli et al., 2005)(Bonaccorsi et al., 2013) and agree with the data obtained in the thermobalance where a weight gain of 0.35% of its initial value has been observed when copper is present. The adsorption of CO_2 over the hydrated sample caused the appearance of a broad and less symmetrical signal with apparent maxima around 1730, 1670, 1550, 1520 and 1460 cm^{-1} superimposed to the band related to the presence of water. Those signals are associated with the formation of bridging, bidentate, monodentate, polydentate and free carbonate species (Danon et al., 2011; Köck et al., 2013; Montanari and Busca, 2008; Villarreal et al., 2017; Westermann et al., 2017, 2015), which were not detected over the sample in dry conditions. The wide variety of carbonate species can be related to several centers, such as copper in different oxidation states previously hydrated and located in the 8 or 6 membered rings, which cannot be completely distinguished. The evolution of the species with the increase in temperature without evacuation was studied by FTIR and the resulting spectra are shown in Figure 9, where the strength and population of these species is evidenced.

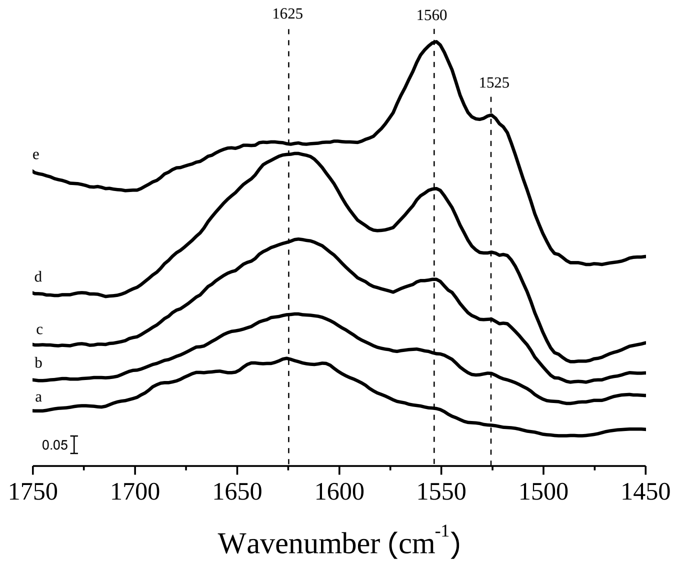

Figure 9. FTIR spectra over 2Cu-SAPO-34 after the co-adsorption of H_2O and CO_2 at a) 200, b) 300, c) 350 and d) 400 ºC and e) after outgassing the sample.

At higher temperatures, signals with maximum at 1625, 1560 and 1525 cm^{-1} that correspond to carbonate-like or hydrogencarbonate species are still present. These signals remained until evacuation of around 400 ºC, indicating similar strength to adsorbed ammonia species (Cortés-Reyes et al., 2016). It is remarkable to note that the carbonation capacity further depends on the hydration of the sample. The interaction between copper species and water and CO_2 would be associated with isolated Cu^+ species preferentially in tetrahedral coordination (Bates et al., 2014), as Cu^+-H_2O-CO_2 stabilized species and Cu^{2+} species in octahedral coordination as part of the structure, which would be prone to higher hydration and carbonation producing azurite-like species ($Cu_3(CO_3)_2(OH)_2$) (Gao et al., 2013; Godiksen et al., 2014).

The mechanism of SCR of NO with NH_3 in presence of O_2, H_2O and CO_2 essentially does not change and the presence of both Cu^+ and Cu^{2+} ions are also visible under SCR conditions. Standard SCR is associated with Cu-redox chemistry requiring NH_3 and NO+O_2; in similar way that in H_2O+CO_2 atmosphere, where the Cu(II) and Cu(I) species are in equilibrium, as copper hydrated carbonated species; these types of copper species are able to react with NO and ammonia to form nytrosil and NH_4^+ intermediates as key species in the SCR process (Cortés-Reyes et al., 2016).

The efficiency of Cu-CHA catalyst in the SCR-DeNO$_x$ process in H_2O+CO_2 conditions is also associated with the increase in the nitrogen selectivity due to the decrease of the N_2O production. In agreement with the bibliography (Grossale et al., 2009), the N_2O formation is caused by the decomposition of surface nitrates, which in the presence of water and CO_2 increase their stability and inhibit their decomposition or the centers for their production are covered. In these conditions, dinuclear Cu species that facilitate nitrate decomposition with N_2O formation were not detected. The reducibility of the tetrahedral Cu^{2+} species is favored in the presence of water, as has been observed over Cu-SSZ-13 synthesized by ion-exchange (Hun Kwak et al., 2012), probably due to the fact that the migration of copper species decreases the bond strength between Cu^{2+} species and the oxygen atoms of the SAPO-34 skeleton and makes the reduction of the adsorbed species faster. In the simultaneous presence of CO_2 and water, Cu^+ and Cu^{2+}-hydrated-carbonated higher coordination species located within CHA-structure, are visible and are responsible for the improvement in the standard SCR. Additionally in these conditions and at low temperatures the standard NH_3-SCR reaction is much faster than ammonia oxidation and was the main reaction in any atmosphere, increasing the conversion values in the presence of water+CO_2. At high temperatures, N_2O formation was observed due to the nitrate decomposition, and ammonia oxidation took place largely under dry conditions. However, the presence of water+CO_2 modifies the Cu-speciation with the formation of Cu^{2+}-H_2O-CO_2 and Cu^+-H_2O-CO_2 species that are apparently responsible for the SCR-performance because these species favor the inhibition of coupled processes, being completely selective to nitrogen in the whole SCR range.

4. Conclusions

Cu-SAPO-34 model SCR catalysts synthesized in one pot with 2wt% of copper inside the framework are hydrothermally stable and the migration of copper to octahedral coordination slightly widens the unit cell. CO_2 is not adsorbed in dry conditions; however, 40 µmol of $CO_2 \cdot g_{cat}^{-1}$ can be adsorbed over the previously hydrated catalyst, via different carbonate species, such as bridging, bidentate, monodentate or polydentate when copper is present in the formulation. NH_3-TPD experiments under different atmospheres allowed the detection of a decrease in the ammonia storage capacity in the presence of water+CO_2, which has been justified due to the cooperative competition between the ammonia and water adsorption and/or CO_2 carbonation over the same sites. Copper species coordination is modified by the reaction atmosphere and the species are directly involved in the redox chemistry of the SCR-process. This material has proven to be efficiently selective to nitrogen because of the inhibition of nitrate decomposition and, in addition, ammonia oxidation is hindered in the SCR technology under *quasi*-real conditions ($1.5\%H_2O+0.3\%CO_2$) in the whole SCR operation temperature range; ensuring NO_x conversion values around 80% and total selectivity to nitrogen.

Acknowledgements

MCR acknowledges the Spanish Ministry of Education, Culture and Sport (FPU12/03826) for the FPU grant and Universidad de Málaga. Campus de Excelencia Internacional Andalucía Tech. The authors want to thank the financial support of the CTQ 2013-47853R Project. Special thanks to Prof Luca Lietti and the LCCP Research Group from Politecnico di Milano for the replication of the catalytic activity experiments in their facilities.

References

Álvaro-Muñoz, T., Márquez-Álvarez, C., Sastre, E., 2012. Use of different templates on SAPO-34 synthesis: Effect on the acidity and catalytic activity in the MTO reaction. Catal. Today 179, 27–34. https://doi.org/10.1016/j.cattod.2011.07.038

Andonova, S., Vovk, E., Sjöblom, J., Ozensoy, E., Olsson, L., 2014. Chemical deactivation by phosphorous under lean hydrothermal conditions over Cu/BEA NH3-SCR catalysts. Appl. Catal. B Environ. 147, 251–263. https://doi.org/10.1016/j.apcatb.2013.08.041

Bates, S.A., Verma, A.A., Paolucci, C., Parekh, A.A., Anggara, T., Yezerets, A., Schneider, W.F., Miller, J.T., Delgass, W.N., Ribeiro, F.H., 2014. Identification of the active Cu site in standard selective catalytic reduction with ammonia on Cu-SSZ-13. J. Catal. 312, 87–97. https://doi.org/10.1016/j.jcat.2014.01.004

Biesinger, M.C., Lau, L.W.M., Gerson, A.R., Smart, R.S.C., 2010. Resolving surface chemical states in XPS analysis of first row transition metals, oxides and hydroxides: Sc, Ti, V, Cu and Zn. Appl. Surf. Sci. 257, 887–898. https://doi.org/10.1016/j.apsusc.2010.07.086

Blakeman, P.G., Burkholder, E.M., Chen, H.-Y., Collier, J.E., Fedeyko, J.M., Jobson, H., Rajaram, R.R., 2014. The role of pore size on the thermal stability of zeolite supported Cu SCR catalysts. Catal. Today 231, 56–63. https://doi.org/10.1016/j.cattod.2013.10.047

Bonaccorsi, L., Calabrese, L., Freni, A., Proverbio, E., 2013. Hydrothermal and microwave synthesis of SAPO (CHA) zeolites on aluminium foams for heat pumping applications. Microporous Mesoporous Mater. 167, 30–37. https://doi.org/10.1016/j.micromeso.2012.06.006

Bonzi, R., Lietti, L., Castoldi, L., Forzatti, P., 2010. NOx removal over a double-bed NSR-SCR reactor configuration. Catal. Today 151, 376–385. https://doi.org/10.1016/j.cattod.2010.02.003

Bordiga, S., Regli, L., Lamberti, C., Zecchina, A., Bjørgen, M., Lillerud, K.P., 2005. FTIR Adsorption Studies of H2O and CH3OH in the Isostructural H-SSZ-13 and H-SAPO-34 : Formation of H-Bonded Adducts and Protonated Clusters. J. Phys. Chem. B 109, 7724–7732.

Brandenberger, S., Kröcher, O., Tissler, A., Althoff, R., 2008. The State of the Art in Selective Catalytic Reduction of NOx by Ammonia Using Metal-Exchanged Zeolite Catalysts, Catalysis Reviews. https://doi.org/10.1080/01614940802480122

Busca, G., Lietti, L., Ramis, G., Berti, F., 1998. Chemical and mechanistic aspects of the selective catalytic reduction of NOx by ammonia over oxide catalysts: A review. Appl. Catal. B Environ. 18, 1–36. https://doi.org/10.1016/S0926-3373(98)00040-X

Can, F., Courtois, X., Berland, S., Seneque, M., Royer, S., Duprez, D., 2015. Composition dependent performance of alumina-based oxide supported WO3 catalysts for the NH3-SCR reaction and the NSR + SCR coupled process. Catal. Today 257, 41–50. https://doi.org/10.1016/j.cattod.2015.03.024

Cao, Y., Zou, S., Lan, L., Yang, Z., Xu, H., Lin, T., Gong, M., Chen, Y., 2015. Promotional effect of Ce on Cu-SAPO-34 monolith catalyst for selective catalytic reduction of NOx with ammonia. J. Mol. Catal. A Chem. 398, 304–311. https://doi.org/10.1016/j.molcata.2014.12.020

Chen, B., Xu, R., Zhang, R., Liu, N., 2014. Economical way to synthesize SSZ-13 with abundant ion-exchanged Cu+ for an extraordinary performance in selective catalytic reduction (SCR) of NOx by ammonia. Environ. Sci. Technol. 48, 13909–13916. https://doi.org/10.1021/es503707c

Chen, P., Rauch, D., Weide, P., Schönebaum, S., Simons, T., Muhler, M., Moos, R., Simon, U., 2016. The effect of Cu and Fe cations on NH3-supported proton transport in

DeNOx-SCR zeolite catalysts. Catal. Sci. Technol. https://doi.org/10.1039/C6CY00452K

Cheng, X., Bi, X.T., 2014. A review of recent advances in selective catalytic NOx reduction reactor technologies. Particuology 16, 1–18. https://doi.org/10.1016/j.partic.2014.01.006

Colombo, M., Nova, I., Tronconi, E., 2012a. Detailed kinetic modeling of the NH3–NO/NO2 SCR reactions over a commercial Cu-zeolite catalyst for Diesel exhausts after treatment. Catal. Today 197, 243–255. https://doi.org/10.1016/j.cattod.2012.09.002

Colombo, M., Nova, I., Tronconi, E., 2012b. NO2 adsorption on Fe- and Cu-zeolite catalysts: The effect of the catalyst red–ox state. Appl. Catal. B Environ. 111–112, 433–444. https://doi.org/10.1016/j.apcatb.2011.10.031

Colombo, M., Nova, I., Tronconi, E., 2010. A comparative study of the NH3-SCR reactions over a Cu-zeolite and a Fe-zeolite catalyst. Catal. Today 151, 223–230. https://doi.org/10.1016/j.cattod.2010.01.010

Cortés-Reyes, M., Finocchio, E., Herrera, C., Larrubia, M.A., Alemany, L.J., Busca, G., 2017. A study of Cu-SAPO-34 catalysts for SCR of NOx by ammonia. Microporous Mesoporous Mater. 241, 258–265. https://doi.org/10.1016/j.micromeso.2016.11.032

Cortés-Reyes, M., Herrera, M.C., Larrubia, M.A., Alemany, L.J., 2016. Fast ultrasound assisted synthesis of Cu-SAPO-34 for SCR application. Int. J. Innov. Res. Sci. Eng. Technol. 5, 5540–5550. https://doi.org/10.15680/IJIRSET.2016.0504189

Cui, Y., Zhang, Q., He, J., Wang, Y., Wei, F., 2013. Pore-structure-mediated hierarchical SAPO-34: Facile synthesis, tunable nanostructure, and catalysis applications for the conversion of dimethyl ether into olefins. Particuology 11, 468–474. https://doi.org/10.1016/j.partic.2012.12.009

Dang, T.T.H., Zubowa, H.-L., Bentrup, U., Richter, M., Martin, A., 2009. Microwave-assisted synthesis and characterization of Cu-containing AlPO4-5 and SAPO-5. Microporous Mesoporous Mater. 123, 209–220. https://doi.org/10.1016/j.micromeso.2009.04.003

Danon, A., Stair, P.C., Weitz, E., 2011. FTIR Study of CO2 Adsorption on Amine-Grafted SBA-15: Elucidation of Adsorbed Species. J. Phys. Chem. C 115, 11540–11549.

De La Torre, U., Pereda-Ayo, B., González-Velasco, J.R., 2012. Cu-zeolite NH3-SCR catalysts for NOx removal in the combined NSR–SCR technology. Chem. Eng. J. 207–208, 10–17. https://doi.org/10.1016/j.cej.2012.06.092

De La Torre, U., Pereda-Ayo, B., Moliner, M., González-Velasco, J.R., Corma, A., 2016a. Cu-zeolite catalysts for NOx removal by selective catalytic reduction with NH3 and coupled to NO storage/reduction monolith in diesel engine exhaust aftertreatment systems. Appl. Catal. B Environ. 187, 419–427. https://doi.org/10.1016/j.apcatb.2016.01.020

De La Torre, U., Urrutxua, M., Pereda-Ayo, B., González-Velasco, J.R., 2016b. On the Cu species in Cu/beta catalysts related to DeNOx performance of coupled NSR-SCR technology using sequential monoliths and dual-layer monolithic catalysts. Catal. Today 273, 72–82. https://doi.org/10.1016/j.cattod.2016.02.054

Duan, Y., Wang, J., Yu, T., Shen, M., Wang, J., 2015. The role and activity of various adsorbed ammonia species on Cu/SAPO-34 catalyst during passive-SCR process. RSC Adv. 5, 14103–14113. https://doi.org/10.1039/c4ra13984d

Fan, S., Xue, J., Yu, T., Fan, D., Hao, T., Shen, M., Li, W., 2013. The effect of synthesis methods on Cu species and active sites over Cu/SAPO-34 for NH3-SCR reaction. Catal. Sci. Technol. 3, 2357–2364. https://doi.org/10.1039/c3cy00267e

Gao, F., Kwak, J.H., Szanyi, J., Peden, C.H.F., 2013. Current understanding of Cu-Exchanged Chabazite molecular sieves for use as commercial diesel engine DeNOx catalysts. Top. Catal. 56, 1441–1459. https://doi.org/10.2800/51626

Gao, F., Mei, D., Wang, Y., Szanyi, J., Peden, C.H.F., 2017. Selective Catalytic Reduction over Cu/SSZ-13: Linking Homo- and Heterogeneous Catalysis. J. Am. Chem. Soc. 139, 4935–4942. https://doi.org/10.1021/jacs.7b01128

Gao, F., Walter, E.D., Washton, N.M., Szanyi, J., Peden, C.H.F., 2015. Synthesis and evaluation of Cu/SAPO-34 catalysts for NH3-SCR 2 : Solid-state ion exchange and one-pot synthesis. Appl. Catal. B Environ. 162, 501–514. https://doi.org/10.1016/j.apcatb.2014.07.029

Godiksen, A., Stappen, F.N., Vennestrøm, P.N.R., Giordanino, F., Rasmussen, S.B., Lundegaard, L.F., Mossin, S., 2014. Coordination Environment of Copper Sites in Cu-CHA Zeolite Investigated by Electron Paramagnetic Resonance. J. Phys. Chem. C 118, 23126–23138. https://doi.org/10.1021/jp5065616

Grossale, A., Nova, I., Tronconi, E., 2009. Ammonia blocking of the "Fast SCR" reactivity over a commercial Fe-zeolite catalyst for Diesel exhaust aftertreatment. J. Catal. 265, 141–147. https://doi.org/10.1016/j.jcat.2009.04.014

Heo, I., Lee, Y., Nam, I.-S., Choung, J.W., Lee, J.-H., Kim, H.-J., 2011. Effect of hydrocarbon slip on NO removal activity of CuZSM5, FeZSM5 and V2O5/TiO2 catalysts by NH3. Microporous Mesoporous Mater. 141, 8–15. https://doi.org/10.1016/j.micromeso.2010.02.005

Hun Kwak, J., Zhu, H., Lee, J.H., Peden, C.H.F., Szanyi, J., 2012. Two different cationic positions in Cu-SSZ-13? Chem. Commun. 48, 4758–4760. https://doi.org/10.1039/c2cc31184d

Kim, Y.J., Kwon, H.J., Heo, I., Nam, I.-S., Cho, B.K., Choung, J.W., Cha, M.-S., Yeo, G.K., 2012. Mn–Fe/ZSM5 as a low-temperature SCR catalyst to remove NOx from diesel engine exhaust. Appl. Catal. B Environ. 126, 9–21. https://doi.org/10.1016/j.apcatb.2012.06.010

Kim, Y.J., Lee, J.K., Min, K.M., Hong, S.B., Nam, I.-S., Cho, B.K., 2014. Hydrothermal stability of CuSSZ13 for reducing NOx by NH3. J. Catal. 311, 447–457. https://doi.org/10.1016/j.jcat.2013.12.012

Köck, E.-M., Kogler, M., Bielz, T., Klötzer, B., Penner, S., 2013. In Situ FT-IR Spectroscopic Study of CO2 and CO Adsorption on Y2O3 ,ZrO2, and Yttria-Stabilized ZrO2. J. Phys. Chem. C 117, 17666–17673.

Leistner, K., Olsson, L., 2015. Deactivation of Cu/SAPO-34 during low-temperature NH3-SCR. Appl. Catal. B Environ. 165, 192–199. https://doi.org/10.1016/j.apcatb.2014.09.067

Lindholm, A., Sjövall, H., Olsson, L., 2010. Reduction of NOx over a combined NSR and SCR system. Appl. Catal. B Environ. 98, 112–121. https://doi.org/10.1016/j.apcatb.2010.05.019

Liu, X., Wu, X., Weng, D., Si, Z., Ran, R., 2016. Evolution of copper species on Cu/SAPO-34 SCR catalysts upon hydrothermal aging. Catal. Today. https://doi.org/10.1016/j.cattod.2016.05.021

Ma, L., Cheng, Y., Cavataio, G., McCabe, R.W., Fu, L., Li, J., 2014. In situ DRIFTS and temperature-programmed technology study on NH3-SCR of NOx over Cu-SSZ-13 and Cu-SAPO-34 catalysts. Appl. Catal. B Environ. 156–157, 428–437. https://doi.org/10.1016/j.apcatb.2014.03.048

Martínez-Franco, R., Moliner, M., Concepcion, P., Thogersen, J.R., Corma, A., 2014. Synthesis, characterization and reactivity of high hydrothermally stable Cu-SAPO-34 materials prepared by "one-pot" processes. J. Catal. 314, 73–82. https://doi.org/10.1016/j.jcat.2014.03.018

Martínez-Franco, R., Moliner, M., Franch, C., Kustov, A., Corma, A., 2012. Rational direct synthesis methodology of very active and hydrothermally stable Cu-SAPO-34 molecular sieves for the SCR of NOx. Appl. Catal. B Environ. 127, 273–280. https://doi.org/10.1016/j.apcatb.2012.08.034

Martini, A., Borfecchia, E., Lomachenko, K.A., Pankin, I.A., Negri, C., Berlier, G., Beato, P., Falsig, H., Bordiga, S., Lamberti, C., 2017. Composition-driven Cu-speciation and reducibility in Cu-CHA zeolite catalysts: a multivariate XAS/FTIR approach to complexity. Chem. Sci. 8, 6836–6851. https://doi.org/10.1039/c7sc02266b

Mihai, O., Widyastuti, C.R., Andonova, S., Kamasamudram, K., Li, J., Joshi, S.Y., Currier, N.W., Yezerets, A., Olsson, L., 2014. The effect of Cu-loading on different reactions involved in NH3-SCR over Cu-BEA catalysts. J. Catal. 311, 170–181. https://doi.org/10.1016/j.jcat.2013.11.016

Montanari, T., Busca, G., 2008. On the mechanism of adsorption and separation of CO2 on LTA zeolites : An IR investigation. Vib. Spectrosc. 46, 45–51. https://doi.org/10.1016/j.vibspec.2007.09.001

Mrad, R., Aissat, A., Cousin, R., Courcot, D., Siffert, S., 2015. Catalysts for NOx selective catalytic reduction by hydrocarbons (HC-SCR). Appl. Catal. A Gen. 504, 542–548. https://doi.org/10.1016/j.apcata.2014.10.021

Niu, C., Shi, X., Liu, F., Liu, K., Xie, L., You, Y., He, H., 2016. High hydrothermal stability of Cu–SAPO-34 catalysts for the NH3-SCR of NOx. Chem. Eng. J. 294, 254–263. https://doi.org/10.1016/j.cej.2016.02.086

Palella, B.I., Cadoni, M., Frache, A., Pastore, H.O., Pirone, R., Russo, G., Coluccia, S., Marchese, L., 2003. On the hydrothermal stability of CuAPSO-34 microporous catalysts for N2O decomposition: A comparison with CuZSM-5. J. Catal. 217, 100–106. https://doi.org/10.1016/S0021-9517(03)00033-2

Paolucci, C., Khurana, I., Parekh, A.A., Li, S., Shih, A.J., Li, H., Di Iorio, J.R., Albarracin-caballero, J.D., Yezerets, A., Miller, J.T., Delgass, W.N., Ribeiro, F.H., Schneider, W.F., Gounder, R., 2017. Dynamic multinuclear sites formed by mobilized copper ions in NOx selective catalytic reduction. Science (80-.). 357, 898–903.

Pereda-Ayo, B., De La Torre, U., Illán-Gómez, M.J., Bueno-López, A., González-Velasco, J.R., 2014. Role of the different copper species on the activity of Cu/zeolite catalysts for SCR of NOx with NH3. Appl. Catal. B Environ. 147, 420–428. https://doi.org/10.1016/j.apcatb.2013.09.010

Petitto, C., Delahay, G., 2015. Selective catalytic reduction of NOx by NH3 on Cu-SAPO-34 catalysts: Influence of silicium content on the activity of calcined and hydrotreated samples. Chem. Eng. J. 264, 404–410. https://doi.org/10.1016/j.cej.2014.11.111

Regli, L., Bordiga, S., Zecchina, A., Bjørgen, M., Lillerud, K.P., 2005. Acidity properties of CHA-zeolites (SAPO-34 and SSZ-13): an FTIR spectroscopic study. Stud. Surf. Sci. Catal. 155, 471–479.

Rutkowska, M., Piwowarska, Z., Micek, E., Chmielarz, L., 2015. Hierarchical Fe-, Cu- and Co-Beta zeolites obtained by mesotemplate-free method. Part I: Synthesis and catalytic activity in N2O decomposition. Microporous Mesoporous Mater. 209, 54–65. https://doi.org/10.1016/j.micromeso.2014.10.011

Shen, M., Wen, H., Hao, T., Yu, T., Fan, D., Wang, J., Li, W., Wang, J., 2015. Deactivation mechanism of SO2 on Cu/SAPO-34 NH3-SCR catalysts: structure and active Cu2+. Catal. Sci. Technol. 5, 1741–1749. https://doi.org/10.1039/c4cy01129e

Shwan, S., Jansson, J., Korsgren, J., Olsson, L., Skoglundh, M., 2012. Kinetic modeling of H-BEA and Fe-BEA as NH3-SCR catalysts—Effect of hydrothermal treatment. Catal. Today 197, 24–37. https://doi.org/10.1016/j.cattod.2012.06.014

Su, W., Li, Z., Peng, Y., Li, J., 2015. Correlation of the changes in framework and active Cu sites for typical Cu/CHA Zeolite (SSZ-13 and SAPO-34) during hydrothermal aging. Phys. Chem. Chem. Phys. 17, 29142–29149. https://doi.org/10.1039/c5cp05128b

Turco, M., Bagnasco, G., Costantino, U., Marmottini, F., Montanari, T., Ramis, G., Busca, G., 2004. Production of hydrogen from oxidative steam reforming of methanol. I. Preparation and characterization of Cu/ZnO/Al2O3 catalysts from a hydrotalcite-like LDH precursor. J. Catal. 228, 43–55. https://doi.org/10.1016/j.jcat.2004.08.026

Villarreal, A., Garbarino, G., Riani, P., Finocchio, E., Bosio, B., Ramírez, J., Busca, G., 2017. Adsorption and separation of CO2 from N2-rich gas on zeolites: Na-X faujasite vs Na-mordenite. J. CO2 Util. 19, 266–275. https://doi.org/10.1016/j.jcou.2017.03.021

Wang, D., Jangjou, Y., Liu, Y., Sharma, M.K., Luo, J., Li, J., Kamasamudram, K., Epling, W.S., 2015. A comparison of hydrothermal aging effects on NH3-SCR of NOx over Cu-SSZ-13 and Cu-SAPO-34 catalysts. Appl. Catal. B Environ. 165, 438–445. https://doi.org/10.1016/j.apcatb.2014.10.020

Wang, D., Zhang, L., Kamasamudram, K., Epling, W.S., 2013. In situ-DRIFTS study of selective catalytic reduction of NOx by NH3 over Cu-exchanged SAPO-34. ACS Catal. 3, 871–881. https://doi.org/10.1021/cs300843k

Wang, D., Zhang, L., Li, J., Kamasamudram, K., Epling, W.S., 2014. NH3-SCR over Cu/SAPO-34 – Zeolite acidity and Cu structure changes as a function of Cu loading. Catal. Today 231, 64–74. https://doi.org/10.1016/j.cattod.2013.11.040

Wang, J., Fan, D., Yu, T., Wang, J., Hao, T., Hu, X., Shen, M., Li, W., 2015. Improvement of low-temperature hydrothermal stability of Cu/SAPO-34 catalysts by Cu^{2+} species. J. Catal. 322, 84–90. https://doi.org/10.1016/j.jcat.2014.11.010

Wang, J., Huang, Y., Yu, T., Zhu, S., Shen, M., Li, W., Wang, J., 2014. The migration of Cu species over Cu-SAPO-34 and its effect on NH3 oxidation at high temperature. Catal. Sci. Technol. 4, 3004–3012. https://doi.org/10.1039/c4cy00451e

Wang, J., Yu, T., Wang, X., Qi, G., Xue, J., Shen, M., Li, W., 2012. The influence of silicon on the catalytic properties of Cu/SAPO-34 for NOx reduction by ammonia-SCR. Appl. Catal. B Environ. 127, 137–147. https://doi.org/10.1016/j.apcatb.2012.08.016

Wang, L., Gaudet, J.R., Li, W., Weng, D., 2013. Migration of Cu species in Cu/SAPO-34 during hydrothermal aging. J. Catal. 306, 68–77. https://doi.org/10.1016/j.jcat.2013.06.010

Westermann, A., Azambre, B., Bacariza, M.C., Grac, I., Ribeiro, M.F., Lopes, J.M., 2017. The promoting effect of Ce in the CO2 methanation performances on NiUSY zeolite : A FTIR In Situ/Operando study. Catal. Today 283, 74–81. https://doi.org/10.1016/j.cattod.2016.02.031

Westermann, A., Azambre, B., Bacariza, M.C., Grac, I., Ribeiro, M.F., Lopes, J.M., Henriques, C., 2015. Insight into CO2 methanation mechanism over NiUSY zeolites : An operando IR study. Appl. Catal. B Environ. 174–175, 120–125. https://doi.org/10.1016/j.apcatb.2015.02.026

Wilken, N., Wijayanti, K., Kamasamudram, K., Currier, N.W., Vedaiyan, R., Yezerets, A., Olsson, L., 2012. Mechanistic investigation of hydrothermal aging of Cu-Beta for ammonia SCR. Appl. Catal. B Environ. 111–112, 58–66. https://doi.org/10.1016/j.apcatb.2011.09.018

Xiang, X., Yang, M., Gao, B., Qiao, Y., Tian, P., Xu, S., Liu, Z., 2016. Direct Cu2+ ion-exchanged into as-synthesized SAPO-34 and its catalytic application in the selective catalytic reduction of NO with NH3. RSC Adv. 6, 12544–12552. https://doi.org/10.1039/c5ra22868a

Yu, T., Hao, T., Fan, D., Wang, J., Shen, M., Li, W., 2014. Recent NH3-SCR Mechanism Research over Cu/SAPO-34 Catalyst. J. Phys. Chem. C 118, 6565–6575.

Yu, T., Wang, J., Shen, M., Li, W., 2013. NH3-SCR over Cu/SAPO-34 catalysts with various acid contents and low Cu loading. Catal. Sci. Technol. 3, 3234–3241. https://doi.org/10.1039/C3CY00453H

Yu, T., Wang, J., Shen, M., Wang, J., Li, W., 2015. The influence of CO2 and H2O on selective catalytic reduction of NO by NH3 over Cu/SAPO-34 catalyst. Chem. Eng. J. 264, 845–855. https://doi.org/10.1016/j.cej.2014.12.017

Zabilskiy, M., Djinović, P., Erjavec, B., Dražić, G., Pintar, A., 2015. Small CuO clusters on CeO2 nanospheres as active species for catalytic N2O decomposition. Appl. Catal. B Environ. 163, 113–122. https://doi.org/10.1016/j.apcatb.2014.07.057

***Declaration of Interest Statement**

Declaration of interests

☒ The authors declare that they have no known competing financial interests or personal relationships that could have appeared to influence the work reported in this paper.

☐The authors declare the following financial interests/personal relationships which may be considered as potential competing interests: